Received: 6 March 2024 | Revised: 25 May 2024 | Accepted: 17 June 2024

DOI: 10.1111/mec.17446

ORIGINAL ARTICLE

MOLECULAR ECOLOGY WILEY

# Exploring Paleogene Tibet's warm temperate environments through target enrichment and phylogenetic niche modelling of Himalayan spiny frogs (Paini, Dicroglossidae)

Sylvia Hofmann[1] | Dennis Rödder[1] | Tobias Andermann[2] | Michael Matschiner[3] | Jendrian Riedel[1] | Chitra B. Baniya[4] | Morris Flecks[1] | Jianhuan Yang[5] | Ke Jiang[6] | Jiang Jianping[6] | Spartak N. Litvinchuk[7] | Sebastian Martin[1] | Rafaqat Masroor[8] | Michael Nothnagel[9] | Vladimir Vershinin[10,11] | Yuchi Zheng[6] | Daniel Jablonski[12] | Joachim Schmidt[13] | Lars Podsiadlowski[1]

[1]Leibniz Institute for the Analysis of Biodiversity Change, Museum Koenig, Bonn, Germany

[2]Evolutionary Biology Centre, Uppsala University, Uppsala, Sweden

[3]Natural History Museum, University of Oslo, Oslo, Norway

[4]Central Department of Botany, Tribhuvan University, Kathmandu, Nepal

[5]Kadoorie Conservation China, Kadoorie Farm and Botanic Garden, Hong Kong, China

[6]Chengdu Institute of Biology, Chinese Academy of Sciences, Chengdu, China

[7]Institute of Cytology of the Russian Academy of Sciences, St. Peterburg, Russia

[8]Pakistan Museum of Natural History, Islamabad, Pakistan

[9]Statistical Genetics and Bioinformatics, Cologne Center for Genomics, University of Cologne, Cologne, Germany

[10]Institute of Plant and Animal Ecology, Ural Branch of the Russian Academy of Sciences, Yekaterinburg, Russia

[11]Institute of Natural Sciences and Mathematics, Eltsyn Ural Federal University, Yekaterinburg, Russia

[12]Department of Zoology, Comenius University in Bratislava, Bratislava, Slovakia

[13]General and Systematic Zoology, Institute of Biosciences, University of Rostock, Rostock, Germany

**Correspondence**
Sylvia Hofmann, Leibniz Institute for the Analysis of Biodiversity Change, Museum Koenig, Bonn D-53113, Germany.
Email: s.hofmann@leibniz-lib.de

**Funding information**
Deutsche Forschungsgemeinschaft, Grant/Award Number: HO 3792/8-1 to SH

**Handling Editor:** Sean D. Schoville

## Abstract

The Cenozoic topographic development of the Himalaya-Tibet orogen (HTO) substantially affected the paleoenvironment and biodiversity patterns of High Asia. However, concepts on the evolution and paleoenvironmental history of the HTO differ massively in timing, elevational increase and sequence of surface uplift of the different elements of the orogen. Using target enrichment of a large set of transcriptome-derived markers, ancestral range estimation and paleoclimatic niche modelling, we assess a recently proposed concept of a warm temperate paleo-Tibet in Asian spiny frogs of the tribe Paini and reconstruct their historical biogeography. That concept was previously developed in invertebrates. Because of their early evolutionary origin, low dispersal capacity, high degree of local endemism, and strict dependence on temperature and humidity, the

Joachim Schmidt and Lars Podsiadlowski contributed equally as senior authors.

cladogenesis of spiny frogs may echo the evolution of the HTO paleoenvironment. We show that diversification of main lineages occurred during the early to Mid-Miocene, while the evolution of alpine taxa started during the late Miocene/early Pliocene. Our distribution and niche modelling results indicate range shifts and niche stability that may explain the modern disjunct distributions of spiny frogs. They probably maintained their (sub)tropical or (warm)temperate preferences and moved out of the ancestral paleo-Tibetan area into the Himalaya as the climate shifted, as opposed to adapting in situ. Based on ancestral range estimation, we assume the existence of low-elevation, climatically suitable corridors across paleo-Tibet during the Miocene along the Kunlun, Qiangtang and/or Gangdese Shan. Our results contribute to a deeper understanding of the mechanisms and processes of faunal evolution in the HTO.

**KEYWORDS**
biogeography, Himalaya, niche modelling, Paini, paleoenvironment, Tibetan Plateau, uplift

## 1 | INTRODUCTION

The Himalaya-Tibet orogen (HTO) is the world's highest and largest mountain system, stretching from the Altyn Tagh and Qilian Mountains at the northeastern margin of the Tibetan Plateau, to the Himalayas in the south, and from the Hengduan Shan at the eastern edge of the Tibetan Plateau to the Hindukush in the far west of the Himalaya. It includes the high plateaus of Tibet and Qinghai, with extensive areas exceeding 4500 m above sea level (a.s.l.). The HTO has a profound impact on the Earth's atmospheric circulation system and Asian biota, so knowing the Cenozoic topographic development of the HTO is essential for exploring the interactions between mountain building, climate, paleoenvironments and biodiversity (Kutzbach et al., 1989; Molnar et al., 2010; Raymo & Ruddiman, 1992; Spicer, 2017; Spicer et al., 2021b; Zhang et al., 2018).

Decades of geoscientific research across the HTO have generated a range of concepts related to its topographic evolution. These concepts differ in the timing, magnitude and sequence of surface uplift of the respective parts of the orogen (reviewed in Spicer et al., 2021b). Many studies, mainly based on stable isotopic paleoaltimetry, provide support for a high Tibetan Plateau as early as the Paleogene, with elevations close to modern values (e.g. Ding et al., 2014; Quade et al., 2011; Rowley & Currie, 2006; Xu et al., 2019), contributing to popular uplift models of the HTO (Fang et al., 2020; Kapp et al., 2007; Mulch & Chamberlain, 2006; Murphy et al., 1997; Spicer et al., 2021b; Tapponnier et al., 2001; Wang et al., 2008, 2014). Other concepts consider the rise of the Plateau to modern elevation exclusively during the Neogene (e.g. Coleman & Hodges, 1995; Harrison et al., 1992; Molnar et al., 1993; Sun et al., 2014; Wang et al., 2006).

Contrasting with the scenario of a highly elevated Paleogene Tibetan Plateau is the fossil record for the Cenozoic HTO (compiled in Schmidt et al., 2023; Spicer et al., 2021a), strongly supporting a lower general topography of significant parts of Tibet with tropical to temperate paleoenvironments until the Early Miocene (reviewed in Ai et al., 2019; Deng et al., 2019). However, insufficient age constraints on the fossil deposits introduce further uncertainties into the chronology of uplift models (Fang et al., 2020; Su et al., 2019). Despite these limitations, no fossils have been unearthed to substantiate the existence of cold temperate or alpine environments in the central and southern HTO during the Paleogene, thereby raising questions about the findings from stable isotope paleoaltimetry (Schmidt et al., 2023).

Organismal evolution, in the sense of dated phylogenies, offers an independent framework for testing historical geography and environmental features (Hoorn et al., 2013; Mulch & Chamberlain, 2018). Recent advances in phylogeographic research in extant Himalayan vertebrates (amphibians: Hofmann et al., 2017, 2019; Hofmann, Jablonski, et al., 2021) and invertebrates (ground beetles: Schmidt et al., 2012) have contributed to our understanding of the paleoenvironmental history of the HTO. Both organismal groups are ideal paleoenvironmental proxies because of the potentially constrained nature of their movements and their dependence on environmental conditions from being ectothermic and adapted to specific microhabitats (e.g. temperature and humidity levels) (Cruz et al., 2024; Pyron, 2014; Schmidt et al., 2017). Amphibians, as well as beetles, show remarkable stability in ecological niches through their evolution, suggesting that dispersal will have been historically constrained to similar climatic zones (Atkinson et al., 1987; Brühl, 1997; Hutter et al., 2013; Schmidt et al., 2011; Wiens, 2011).

Based on the contemporary disjunct distributional patterns and molecular phylogeny of mega-diverse *Carabus* ground beetles, a model of the paleoenvironmental evolution of the HTO has been recently published by Schmidt and colleagues, arguing for a rather young age of cold temperate to alpine biomes in the HTO (Schmidt et al., 2023). This new scenario suggests subtropical or warm temperate environments and, consequently, low average elevations in the orogenetic system until at least the Oligocene-Miocene boundary.

Similar to ground beetles, Himalayan spiny frogs (Paini, Dicroglossidae) exhibit markedly disjunct geographical patterns.

Given the previous age estimates for Paini (Early to Mid-Miocene), these disjunct areas are expected to originate from trans-Tibet dispersal events during the Paleogene and paleo-Tibet's role as a primary evolutionary center for biotas (Hofmann et al., 2019, 2023; Hofmann, Jablonski, et al., 2021). Spiny frogs are a characteristic element of the HTO, occurring from the northern Hindukush in Afghanistan, through western and northern Pakistan, Nepal, Bhutan, northern India including Sikkim, and in the valleys of southern and eastern Tibet, eastwards to eastern China, and southwards to the mountains of Indochina (Myanmar, Thailand, Laos and northern Vietnam; Frost, 2024). According to Frost (2024), the Paini comprise the genus *Nanorana* (34 species), *Quasipaa* (13 species), *Allopaa* (possibly two species; nested within *Nanorana*; see Hofmann, Masroor, et al., 2021; Hofmann et al., 2023) and the monotypic genus *Chrysopaa*. The genus *Nanorana* contains the subgenera *Paa* and *Chaparana*. The spatio-temporal diversification of spiny frog lineages endemic to the Himalayas has been shown to be highly informative of the environmental and uplift history of the HTO (Hofmann et al., 2019; Hofmann, Jablonski, et al., 2021). However, previous phylogenetic inferences of these frogs were based on multilocus datasets showing lower resolution for several clades along the phylogenetic tree (e.g. mito-nuclear discordance, low nodal support values), thus entailing uncertainties in the biogeographic scenario.

Here, we used genomic data, ancestral range estimation and paleoclimatic niche modelling to (re-)assess the historical biogeography of spiny frogs and its linkage to the paleoenvironmental evolution of the HTO. We specifically aim at (i) obtaining a robust and well-resolved dated phylogeny, (ii) investigating whether spiny frogs in the Cenozoic HTO may have retained their ancestral ecological niche characteristics over time or whether they are more likely to have adapted in situ, (iii) reconstructing the history of their geographic range changes over time and (iv) exploring the evolution of the species' disjunct distribution pattern under a scenario of a warm temperate Miocene Tibet.

## 2 | MATERIALS AND METHODS

### 2.1 | Taxon sampling

The taxon set contained 36 samples of the genus *Nanorana*. Furthermore, we included species of the genera *Chrysopaa*, *Quasipaa*, *Hoplobatrachus*, *Euphlyctis*, and *Minervarya*, as well as *Microhyla ornata*, *Ptychadena longirostris*, and *Phrynobatrachus phyllophilus* as outgroups. All tissue samples for molecular work were obtained from museum holdings or came from scientific collections (Chinese Academy of Science, China; Chengdu Institute of Biology, China; Comenius University, Bratislava, Slovakia; Kadoorie Farm and Botanic Garden, Hong Kong; Natural History Museum Basel, Switzerland; Natural History Museum Erfurt, Germany; Russian Academy of Science, Moscow, Russia; Senckenberg Museum, Frankfurt am Main, Germany; Museum Koenig, Bonn, German; Natural History Museum Berlin, Germany). The list of samples and their associated metadata are presented in Table S1. Sample selection was based on distribution patterns and phylogenetic relationships (Hofmann et al., 2019; Hofmann, Jablonski, et al., 2021) to maximize geographic coverage for the taxonomic group and to obtain a representative dataset across the Himalayan region.

### 2.2 | Data generation and assembly

Genome-scale DNA data were produced through selective amplification of target regions with exon capture (Bi et al., 2012; Portik et al., 2016). The required oligonucleotide baits for exon capture were designed based on available transcriptome sequences. Exon alignments, probe design, wet laboratory procedures and handling of raw sequence reads are extensively described in the Supplementary Information Text.

Alignments were generated and processed applying three different approaches: (i) using MeShClust 3.0 (Girgis, 2022) and the resulting sequence clusters as a query to search against the targets, (ii) with SECAPR, using the assembled contigs to search against the target loci and aligning the extracted target contigs with MAFFT (Katoh & Standley, 2013), and (iii) using the assembled contigs as a BLAST query to search against a reference contig among all assembled reads and filtering gene alignments by BMGE (Criscuolo & Gribaldo, 2010) and clock-like evolution using BEAST. Further details are described in Supplementary Information Text.

The three methods MeShClust, SECAPR and BLAST+BEAST produced sets with varying numbers of recovered loci: 468/331/422 (~404/~282/~115 kbp; for length distribution of sequences see Figure S1). For downstream analysis, we additionally used the BMGE processed alignments of the BLAST approach (BLAST+BMGE), which we filtered for potential paralogues/duplicates using a clustering approach with CD-HIT-EST (Li & Godzik, 2006), resulting in 2285 loci (~989 kbp) for the taxon set. An overview of the workflow is presented as flowchart in the Figure S2, and heatmaps of data distribution across the samples are shown in Figure S3.

### 2.3 | Phylogenomic analyses

To assess potential biases arising from different data types and data filtering strategies, we analysed all datasets separately. Phylogenetic estimation was performed using concatenation and summary coalescent-based methods. Based on the concatenated data, we inferred maximum likelihood (ML) phylogenies using IQ-TREE2 v2.1.2 (Minh et al., 2020) with the MFP+MERGE option to assess the optimal gene partition scheme. Nodal support was calculated using ultrafast bootstrap approximation (UFBoot) (Minh et al., 2013) and the Shimodaira-Hasegawa approximate

likelihood ratio test (SH-aLRT) (Guindon et al., 2010) using 10,000 iterations in each case. For the analysis of the dataset with 2285 loci, we applied the GTR+I+G substitution model to each partition and 1000 UFBoot/SH-aLRT replicates. To diminish the risk of overestimating branch supports with UFBoot, we used the –bnni option implemented in IQ-TREE2. Computational burden was reduced by the relaxed hierarchical clustering algorithm (rcluster) (Lanfear et al., 2014) with the rcluster percentage set to 5. For all analyses, three replicate runs were performed. Only nodes with support values of UFBoot ≥ 95 and SH-aLRT ≥ 90 were considered robust. We also performed Bayesian inference of phylogeny using MrBayes v.3.2.7 (Ronquist et al., 2012) on the concatenated datasets partitioned by genes, except for the dataset of 2285 loci, which we analysed both unpartitioned using RevBayes v.1.2.1 (Höhna et al., 2014, 2016) and partitioned by genes with ExaBayes (Aberer et al., 2014). For each MrBayes analysis, we defined a GTR+I+G model for all gene partitions, four runs, four chains with a length of 1 million generations per chain, a sampling frequency of 100, and a burn-in of 25%. Convergence was assessed by the MrBayes built-in diagnostics, namely the average standard deviation of split frequencies (ASDSF; target value 0.05), the potential scale reduction factor (PSRF; target value ≥ 1.0) and the estimated effective sample size (ESS; target value 100). Markov-chain Monte Carlo (MCMC) was performed in two independent replicates for both RevBayes and ExaBayes, with 4 MCMC chains of 50,000 (RevBayes) and 500,000 (ExaBayes) generations, a thinning interval of 100 and 500, respectively, and a burn-in fraction of 25%. A summary species tree was constructed based on the different alignments using ASTRAL-MP v.15.5 (Yin et al., 2019), with gene trees generated by RAxML under the GTRGAMMA (Stamatakis, 2014). Branches were further annotated with quartet support (–*t* 1) to assess gene tree conflicts.

## 2.4 | Species delimitation

The UFBoot-trees generated by IQ-TREE2 for the dataset with 2285 loci were analysed using Bayesian Poisson Tree Processes (bPTP) (Zhang et al., 2013) and 100,000 iterations, a thinning of 100 and a burn-in of 10%. For comparison, we also generated input trees for bPTP with RAxML-NG (Kozlov et al., 2019) using the same gene-partitioned dataset with 2285 loci and applying the GTR-GAMMA model. Nodal support was assessed using Felsenstein bootstrap (fbp) and transfer bootstrap expectation (tbe) based on 1000 replicates. Species delimitation with bPTP was then performed with the same specifications as before. Since bPTP considers the tree structure and branch lengths for delimitation, we removed (out)groups and *Chaparana* that are distantly related to the *Nanorana* and *Paa* groups to avoid biased delimitation results (Zhang et al., 2013). Taxa that were indicated by bPTP to be conspecific based on either the IQ-TREE2 or the RAxML-NG input trees were pruned to one individual per taxon for the niche modelling approach (see below).

## 2.5 | Topology tests

Topology tests were performed in IQ-TREE2 using the approximately unbiased (AU) test (Shimodaira, 2002), tests implementing the RELL approximation (Kishino et al., 1990), the Kishino-Hasegawa test (Kishino & Hasegawa, 1989), the Shimodaira-Hasegawa test (Shimodaira & Hasegawa, 1999) and expected likelihood weights (Strimmer & Rambaut, 2002). Model parameters were estimated based on the maximum likelihood tree from the dataset with 2285 loci, and the number of RELL replicates was set at 1 million. We tested all unique consensus topologies (m0-m3; see Results).

## 2.6 | Divergence time estimation

For estimating divergence dates, we used BEAST2 v. 2.7 (Bouckaert et al., 2019) and the gene dataset selected by SECAPR (Figure S2) because outgroups were sufficiently represented and sequences across loci were longer, and their length distribution more even compared with the other datasets (Figure S1). These multiple sequence alignments (MSAs; one per gene) were further filtered by the presence of outgroups, resulting in 51 loci. The following age constraints were used to calibrate the molecular clock in BEAST2, with a soft upper 95% quantile bound derived from timetree.org: (i) a minimum age of 33.9 my of the most recent common ancestor (MRCA) of Ranoidea, based on the fossil *Thaumastosaurus gezei* (Rage & Rocek, 2007) (soft maximum 120 Ma, lognormal prior); (ii) a minimum age of 25 Ma for the *Ptychadena-Phrynobatrachus* split, based on the earliest Ptychadenidae fossil (Blackburn et al., 2015) (soft maximum 101 Ma, lognormal prior); (iii) the secondary age constraint of 64.2 ± 12.1 Ma for the split between the Paini tribe and other Dicroglossidae (Bossuyt et al., 2006; Che et al., 2010) (normal prior); (iv) the secondary age constraint of 38.1 ± 9.4 Ma for the MRCA of Paini (Bossuyt et al., 2006) (normal prior); and (v) 3.5–9.2 Ma as the 2.5% and 97.5% quantiles of the secondary age constraint for the MRCA of the alpine and subalpine *Nanorana* species *N. parkeri*, *N. pleskei* and *N. ventripunctata* (Hofmann et al., 2019) (the range largely overlaps with previous estimations, e.g. Hedges et al., 2015; Pyron, 2014; Sun et al., 2018) (normal prior).

We performed 100 million Markov-chain Monte Carlo (MCMC) iterations for each of 10 replicate runs sampling every 10,000th iteration, and applied a lognormal relaxed clock model, a birth-death tree prior, a random starting tree and the HKY model with four gamma rate categories for the substitution rate (unlinked between genes). Posterior tree estimates from the replicate runs were combined with BEAST2's LogCombiner v.2.6.2, resampling trees at a lower frequency for a total of ca. 20,000 trees. Convergence and stationarity of MCMC chains were verified with Tracer (Rambaut et al., 2018) and supported by a standard deviation of split frequencies <0.01 as well as an effective sample size value >200 for each parameter. Finally, a maximum-clade-credibility

summary tree with node ages set to mean estimates was obtained with TreeAnnotator v.2.6.2 and visualized with FigTree v.1.4 (Drummond & Rambaut, 2007).

## 2.7 | Species distribution modelling

To assess the potential geographic distribution of the taxa, we computed distribution models using two different approaches: species distribution modelling (SDM) and phylogenetic niche modelling (PNM). The models were computed based on the species' currently occupied climatic niches and subsequently projected onto paleoclimatic scenarios. While our species distribution modelling approach relies on a static characterization of the species' realized niches derived from present-day taxon occurrence data, our phylogenetic niche modelling approach accounts for evolutionary changes by interpolating the realized niches along a phylogeny.

Species locality records associated with geographical coordinates were obtained from our own data (Hofmann et al., 2019, 2023; Hofmann, Jablonski, et al., 2021), Table S1, and GBIF (www.gbif.org); the latter were manually curated for erroneous records. Only species with a minimum number of 10 records (median = 38, max = 184) were considered in the analysis. We downloaded 19 bioclimatic variables for the present time (1979–2013) from the CHELSEA database v.2.1 (Karger et al., 2018) at a resolution of 2.5 arc minutes. To reduce collinearity between variables, we selected only one predictor among pairs with a Spearman's pairwise rank correlation of higher than |0.75|. The final set comprised predictors reflecting thermal energy and water availability relevant for an ectothermic organism (i.e. mean temperature of wettest quarter = bio8, mean temperature of warmest quarter = bio10, mean temperature of coldest quarter = bio11, annual precipitation = bio12, precipitation of the driest month = bio14, precipitation of the warmest quarter = bio18, and precipitation of the coldest quarter = bio19). Paleoclimatic variables for the mid-Pliocene warm period (mPWP v1.0, 3.205 Ma) (Hill, 2015), and mid-Pliocene cooling period (Marine Isotope Stage M2 v1.0, 3.3 Ma) (Dolan et al., 2015) were downloaded with a spatial resolution of 2.5 arc min from the paleoclimate data base (Brown et al., 2018). For SDM calculation and model fitting, we used MaxEnt ver. 3.4.4 (Phillips, Anderson, et al., 2017; Phillips & Dudík, 2008; Phillips, Dudík, & Schapire, 2017) using a model optimization procedure based on AICc as described in Ginal et al. (2022); details are explained in Supplementary Information Text. Potential areas with non-analogous climatic conditions exceeding the training range of the models were identified using multivariate environmental similarity surfaces (Elith et al., 2010).

For phylogenetic niche modelling (PNM), we applied a custom R code based on the R package *machuruku* (Guillory & Brown, 2021).

We first pruned the time-calibrated phylogeny leaving only those species within the group in question (*Allopaa*, *Chrysopaa*, *Nanorana*, and *Quasipaa*), and for which we had enough record data (≥10). For this set of taxa, we constructed present-day potential distribution using the same bioclim variables which we used for SDM computation.

Second, the contemporary response parameters for all taxa and the pruned, time-calibrated phylogeny were used to estimate the ancestral character on each climate response value over the input phylogeny for the particular time slices (mpwp, MIS M2), using the 'ace' function from the R package ape (Paradis et al., 2004), under maximum likelihood with a Brownian motion (BM) model of evolution. Finally, we converted the ancestral climate response parameters into ancestral niche models using the *dsnorm* function in the R package *fGarch* (Wuertz et al., 2019). The reconstructed models were then projected into corresponding paleoclimatic data layers to visualize suitability for that lineage in paleogeographic space.

We pruned the time-calibrated tree before modelling, removing all taxa with uncertain taxon determination (sp., cf.) and using only one representative per taxon (see Figure S4). Although we modelled shifts in ancestral suitable habitat using data from all taxa of our phylogenetic tree for which enough occurrence records are available, we focused our attention here on the most revealing species with a remarkable disjunct distribution and/or which represent a major clade across the phylogeny: *Chrysopaa sternosignata*, *Nanorana* (*Allopaa*) *hazarensis*, *N.* (*Paa*) *vicina*, and *N.* (*Paa*) *blanfordii*.

## 2.8 | Testing for phylogenetic niche conservatism

Phylogenetic signal is generally recognized as the tendency of related species to resemble one another; a strong phylogenetic signal has been interpreted as a sign of niche or evolutionary conservatism (Revell et al., 2008).

Because amphibians are highly sensitive to water availably and environmental temperature (e.g. Beebee, 1995; Pilliod et al., 2022; Pottier et al., 2022), whereby the latter directly depends on topography, that is altitude, we tested for correlations between phylogenetic relatedness and the weighted mean of the annual mean temperature (bio1) and precipitation (bio12) based on the species' potential distribution as computed via predicted niche occupancy profiles (Evans et al., 2009; Heibl & Calenge, 2018). Ancestral states were reconstructed using the *contMap* function in the *phytools* R package (Revell, 2014). We assessed the phylogenetic signals using Blomberg's *K* (Blomberg et al., 2003) and Pagel's $\lambda$ (Freckleton et al., 2002; Pagel, 1999), as implemented in the *phylosig* function in the R package *phytools* (Revell, 2012). Both indices assume a Brownian motion (BM) model of evolution, where a value close to zero indicates phylogenetic independence and a value closer to one indicates a stronger relationship between traits and phylogeny, as expected under BM. The maximum value of Pagel's $\lambda$ is 1, whereas Blomberg's K can take higher values when the signal is stronger than BM. The significance of *K* and $\lambda$ was assessed using a randomization test for *K* and a likelihood ratio test for $\lambda$ ($p \leq .05$ indicates strong evidence against the null hypothesis of no phylogenetic signal).

### 2.9 | Biogeographical analyses

Ancestral range estimations (ARE) were performed with the R package BioGeoBEARS (Matzke, 2013) through common biogeographical models under the recent paleoenvironmental scenario of the HTO, according to Schmidt et al. (2012, 2023). This scenario was implemented by a constrained adjacency and biome-dependent dispersal matrix at certain time slices (see Supplementary Information Text, Figure S5 and Tables S2–S4). We pruned the dated input tree to one individual per taxon and according to the bPTP species delimitation results (Figure S4).

Species' occurrences were coded within 19 geological elements of the HTO (see Figure S5). Since there are no extant species that occupy more than two areas, we restricted ranges to comprise at most two different areas at each node. Three biogeographic models were assessed: (i) Dispersal-Extinction-Cladogenesis (DEC; Ree et al., 2005), (ii) DIVALIKE (modified from the DIVA program; Ronquist, 1997) and (iii) BAYAREALIKE (modified from the BayArea program; Landis et al., 2013). We did not include the + J parameter with any model because of the potential conceptual issues of this method (Ree & Sanmartin, 2018). We selected the best biogeographical model using the AIC and AICc criteria from BioGeoBEARS. To characterize the number and nature of biogeographical events in the best-fitting model, we performed biogeographic stochastic mapping (BSM; Dupin et al., 2016; Matzke, 2016) in BioGeoBEARS using 50 runs. We then tested the confidence of the BSM by comparing the state probabilities with those obtained under a ML model.

## 3 | RESULTS

### 3.1 | Phylogenomic relationships

We provide the first genomic-based, well-resolved phylogeny for spiny frogs of the HTO, with strong support for most clades (Figure 1). In general, two main groups are recovered: a subtropical clade (genera *Chrysopaa* and *Quasipaa*) and a temperate to alpine clade (genus *Nanorana*). The latter comprises six subclades: one from warm temperate regions (subgenera *Chaparana* and *Allopaa*; note, we treat *Allopaa* as subgenus within *Nanorana* to resolve paraphyly, see Hofmann et al., 2023), one from (sub)alpine regions of the Tibetan Plateau and its eastern margins (nominal subgenus *Nanorana*) and four from (cold-) temperate regions of the Greater Himalaya (subgenus *Paa*). Of these four subclades, one represents a species-diverse group in the East Himalaya, one occurs in the Central Himalaya, and

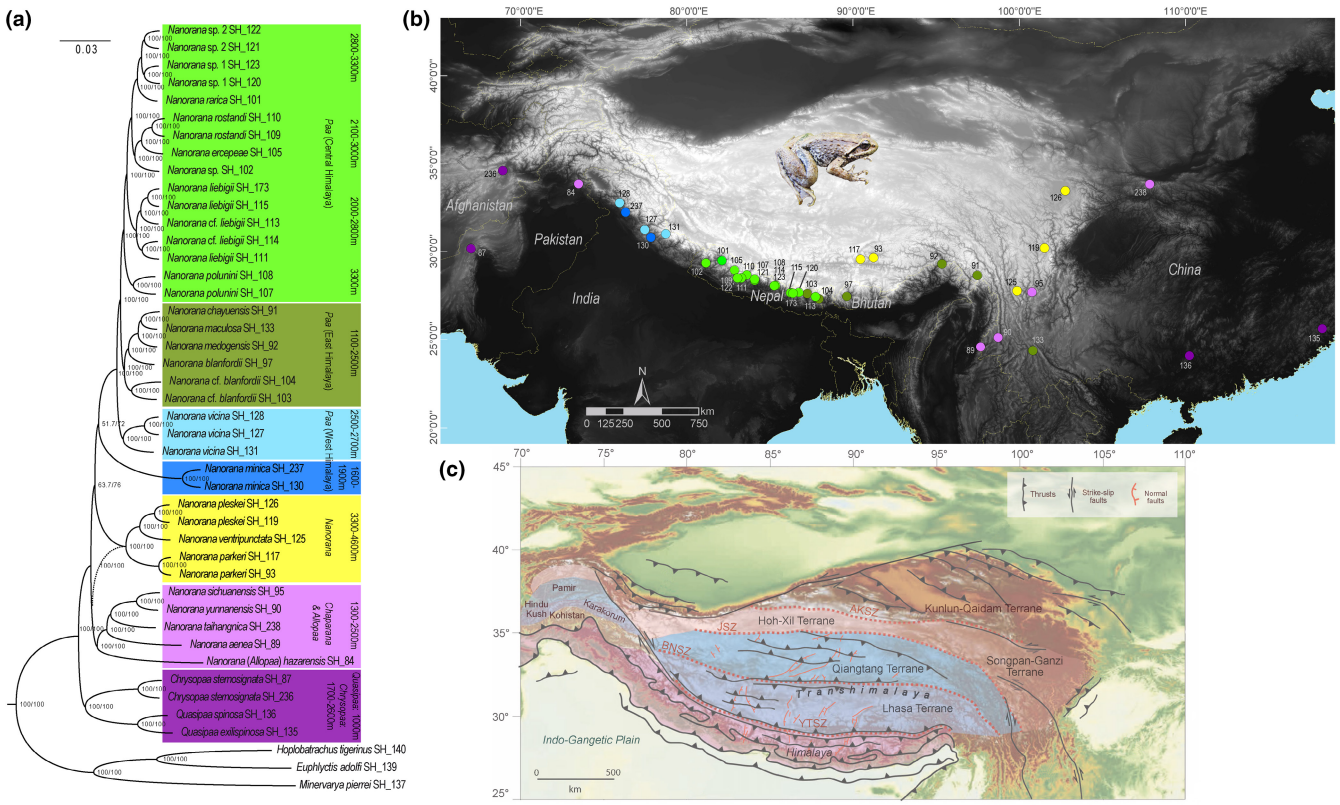


FIGURE 1 Phylogenetic tree (a) inferred with IQ-TREE2 based on 2285 loci, (b) sampling localities of spiny frog species (coloured dots, labelled with sequence ID; see Table S1) with different colours indicating different clades of the tree and (c) geological map of the Himalaya-Tibet region showing the major terranes, suture zones (dotted red lines), thrusts (black lines) and faults (red lines), modified from Spicer et al. (2021a); BNSZ, Bangong–Nujiang Suture Zone; JSZ, Jingsha Suture Zone; KSZ, Kunlun Suture Zone; YTSZ, Yarlung–Tsangpo Suture Zone; Photograph: *Nanorana liebigii* (credit: S. Hofmann).

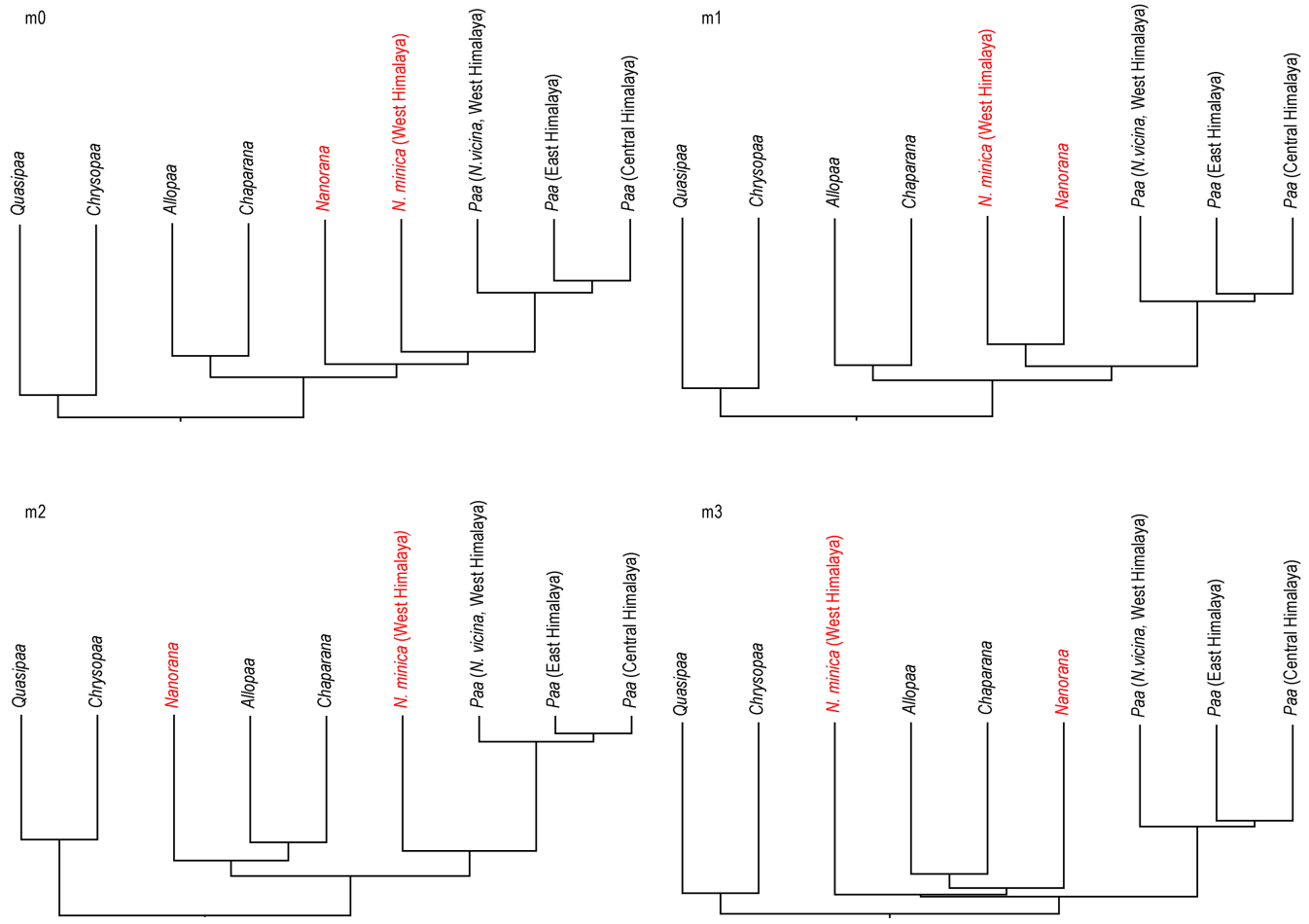


| tree | logL | deltaL | bp-RELL | p-KH | p-SH | p-WKH | p-WSH | c-ELW | p-AU | |
|---|---|---|---|---|---|---|---|---|---|---|
| m0 | -5709748.749 | 0.000 | 0.673 + | 0.674 + | 1 + | 0.674 + | 0.914 + | 0.673 + | 0.673 + | |
| m1 | -5711694.282 | 1945.500 | 0 - | 0 - | 0 - | 0 - | 0 - | 0 - | 1.47e-54 - | rejected |
| m2 | -5709806.054 | 57.305 | 0.327 + | 0.326 + | 0.613 + | 0.326 + | 0.63+ | 0.327 + | 0.327 + | |
| m3 | -5710258.280 | 509.530 | 0 - | 0.00062 - | 0.0114 - | 0 - | 0 - | 1.77e-63 - | 1.03e-05 - | rejected |

m0 = ML/BI: BLAST+BMGE (2,285), MeShClust (468); sp. tree: MeShClust (468)
m1 = ML/BI: BLAST+BEAST (422), SECAPR (331)
m2 = sp. tree: BLAST+BEAST (422), SECAPR (331)
m3 = sp. tree: BLAST+BMGE (2,285)

**FIGURE 2** Placement of nominal subgenus *Nanorana* from (sub)alpine regions and *Nanorana minica*) from West Himalaya in the phylogenetic trees resulting from different analysis. The different analysis types (ML: Maximum likelihood; BI: Bayesian inference; sp. tree: summary species tree) and datasets, followed by the number of loci in brackets, are listed below the table (for tree files see Supplementary Data D1–D14). Topology tests were performed in IQ-TREE 2. DeltaL = logL difference from the maximal logl in the set; bp-RELL = bootstrap proportion using RELL method (Kishino et al., 1990); *p*-KH = *p*-value of one-sided (Kishino & Hasegawa, 1989); *p*-SH = *p*-value of Shimodaira-Hasegawa test (Shimodaira & Hasegawa, 1999). The topologies m1 and m3 are rejected, while m0 and m2 are not. c-ELW = Expected Likelihood Weight (Strimmer & Rambaut, 2002); *p*-AU = *p*-value of approximately unbiased (AU) test (Shimodaira, 2002); plus signs denote the 95% confidence sets; minus signs denote significant exclusion.

two are restricted to the West Himalaya, both of which are represented by a single species (*N. vicina* and *N. minica*; Figure 1).

The resulting trees were mostly consistent across all analyses, irrespective of the method or dataset used (Figures 1, S6, S7, and Supplementary Data D1–14). However, for a few clades, their (in most cases strongly supported) position in the tree recurrently disagreed. Specifically, we recovered different placements for the (sub) alpine *Nanorana* clade (*N. parkeri*, *N. pleskei and N. ventripunctata*) and the clade from the West Himalaya (*N. minica*) (Figure 2). Because the positions of these two clades are meaningful for understanding present-day biogeographic patterns, we performed four different topology tests (see Material and Methods section). Two of them were rejected, the following were not rejected (Figure 1): m0—subgenera *Chaparana* and *Allopaa* form the sister clade to all other *Nanorana*

clades, with the (sub)alpine, nominal subgenus *Nanorana* placed as sister to the subgenus *Paa* and *N. minica*; m2—the nominal subgenus *Nanorana*, is the sister clade to the subgenera *Chaparana* and *Allopaa*, which together constitute the sister clade of the subgenus *Paa* and *N. minica*. In both topologies, *N. minica* is sister to the clades of the subgenus *Paa* from the West, East and Central Himalaya. Therefore, we treat *N. minica* as a member of the subgenus *Paa*.

## 3.2 | Niche stability and niche modelling

The predicted ancestral niche occupancy profiles for the mean annual temperature (bio1) and precipitation (bio12), as well as the ancestral state estimation for both parameters show evidence of phylogenetic niche conservatism in spiny frogs of the HTO (Figure 3). In line with this, we found significant phylogenetic signals under both Blomberg's *K* ($p < .01$) and Pagel's $\lambda$ ($p < .01$) for bio1, and for bio12 under Blomberg's *K* ($p < .01$). The ancestral state phenogram further suggests that the frogs likely diverged from a (warm-) temperate ancestor and that cold-adapted, (sub)alpine lineages did not occur before the Late Miocene (<10 Ma).

Present-day SDMs performed well and displayed high predictive accuracy (see Table S5). In Figure 4, the present and hindcast SDM projections are shown based on both SDM and phylogenetic niche modelling (for projections including MESS areas and for separate presentation of time slices see Figure S8a–d). The present projections largely match the known, disjunct geographic distribution of the respective taxon (Figures 4, S8a–d and S9), but also show (broad) extensions of suitable habitats outside the restricted occurrence range. In *Nanorana hazarensis*, both the SDM

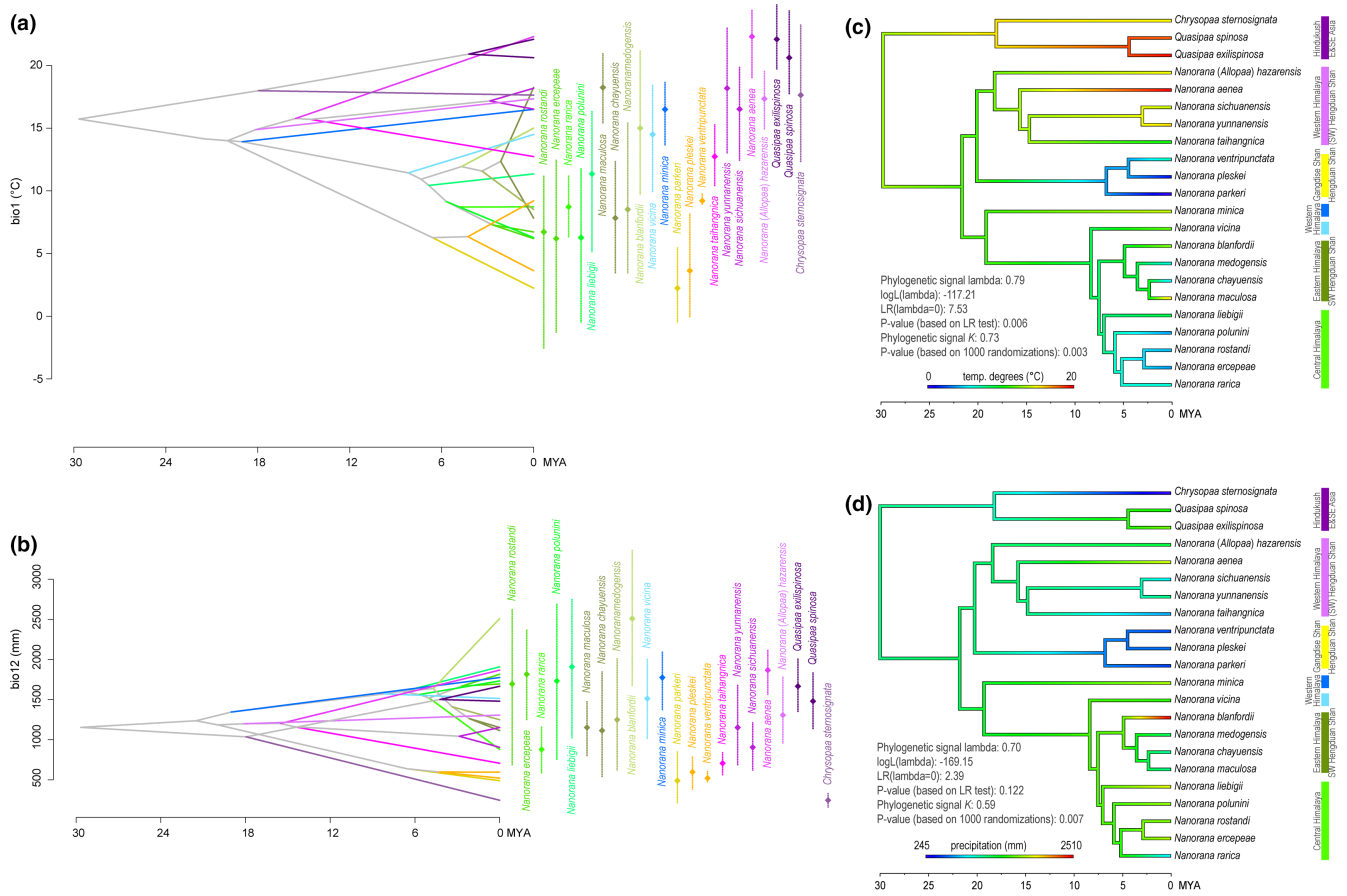


**FIGURE 3** Inferred history of the evolution of environmental niches based on predicted niche occupancy profiles for (a) the annual mean temperature (bio1) and (b) annual precipitation (bio12), and ancestral state estimation of bio1 (c) and bio12 (d) within spiny frogs based on a BEAST2 tree. In (a) and (b), the internal nodes denote the mean of climatic tolerances as estimated for the most recent common ancestor of the related extant taxa. Vertical bars and point marks show the 80% central density of environmental tolerance for each extant taxon and the related mean values, respectively. Lines and points are coloured according to clades defined in Figure 1. In (c) and (d), the measures of the phylogenetic signal, namely Blomberg's *K* and Pagel's $\lambda$, are also presented.

**FIGURE 4** Present and hindcasted SDMs for the four selected species projected over the mid-Pliocene warm period (mPWP), and the Marine Isotope Stage M2 cooling period. Records of the respective species fall within the black dashed line area. (a–d) Based on species distribution modelling; (e–h) based on phylogenetic niche modelling. For projections including MESS layer and separate presentation of each time slice see Figure S8a–d.

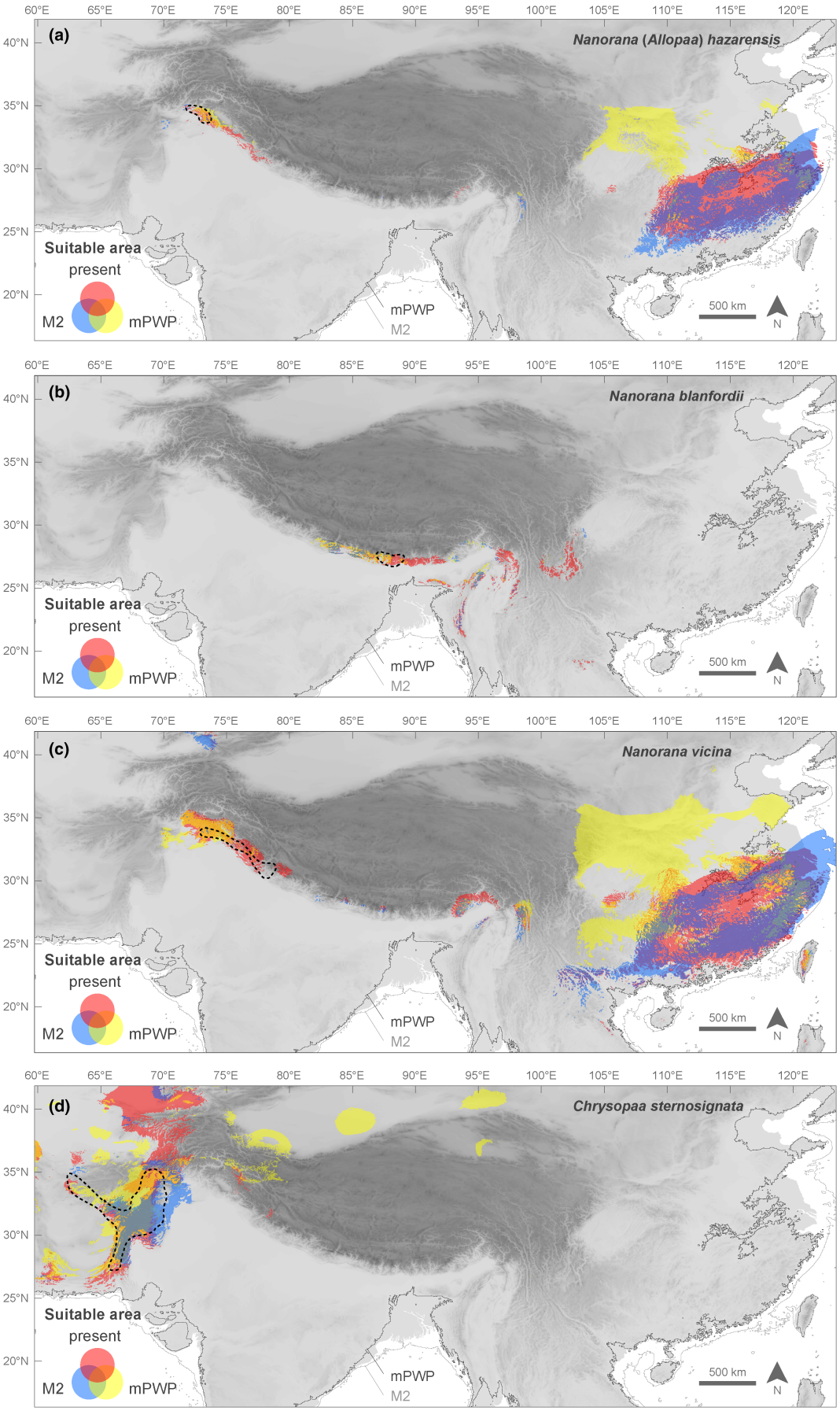

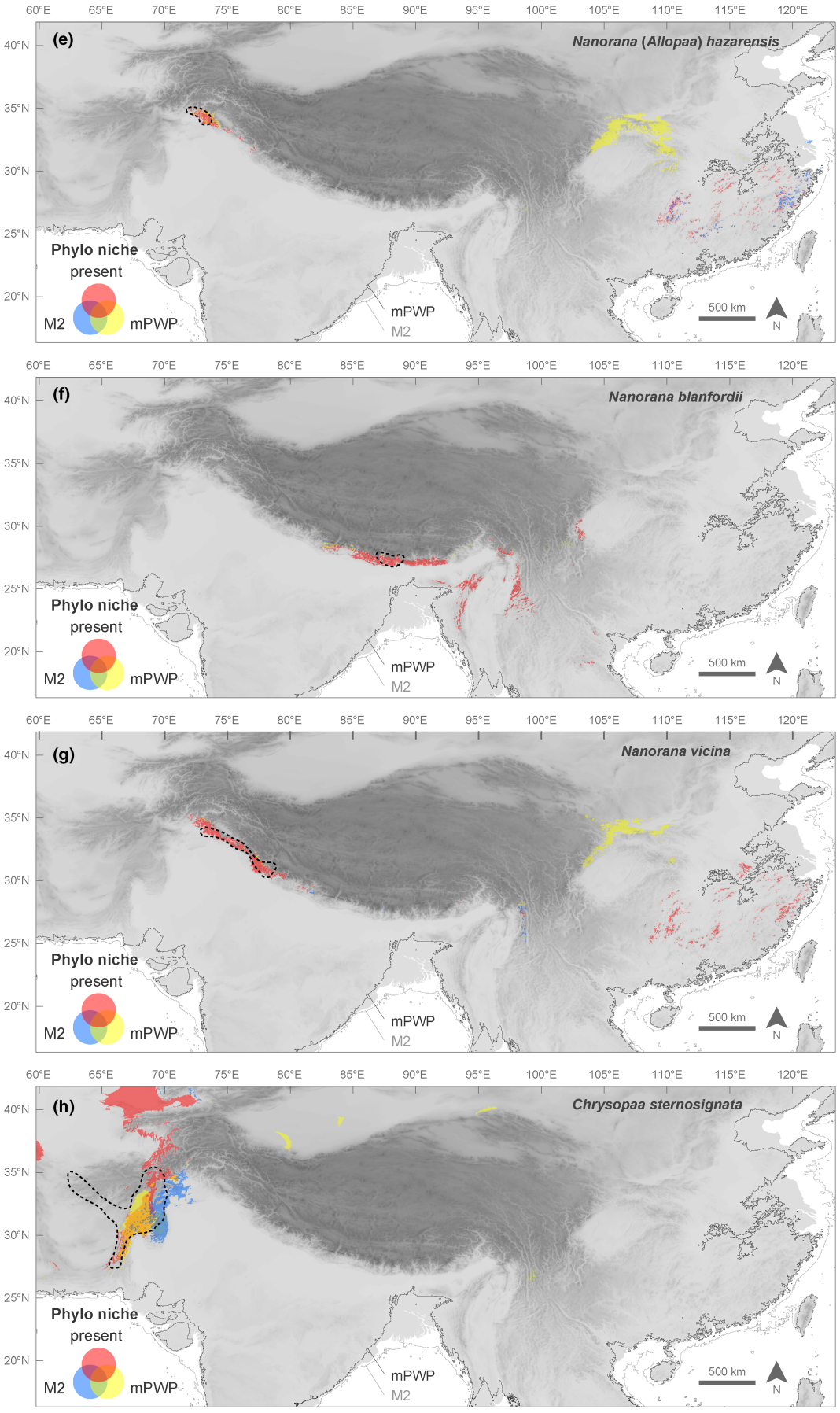


FIGURE 4 (Continued)

projections and phylogenetic niche models over the present time and the cooling period M2 show similar (large-scale) areas of suitable habitats across eastern China and a very small, disjunct (or, based on the SDM projection into M2, non-existing) area in the far West Himalaya, where this taxon is exclusively found. In contrast, projection over the warm mPWP reflects a major shift of suitable areas in China towards northern areas (Qilian Shan; matching the present distribution of the closely related *N. taihangnica*, Figure 9d), and an extension of the disjunct area in the West Himalaya compared with the cool M2 period. Notably, the species' projected range in the West Himalaya shrinks to micro- or non-existing refugia during the cooling event (Figure S8a). Similar results were obtained for the West-Himalayan species *N. vicina*. In *Chrysopaa sternosignata*, present-day and M2 suitable habitats cover similar areas of the Hindukush and, according to the SDM projection, extend to the north of the Alai mountains. During the warm mPWP period, disjunct spots of suitable areas are predicted along the northern margin of Tibet. In *N. blanfordii*, geographic shifts of suitable areas are identified in the Central and East Himalaya between the three time slices and based on SDM projections also in the regions of southwestern Hengduan Shan and western Southeast Asia (Arakan Mts.). However, this species is only known from the high montane regions of the eastern-central and East Himalaya.

We revealed that: (i) potential geographic distribution ranges of the frogs apparently fluctuated strongly in response to past climate changes; (ii) no suitable habitat corridors were predicted for the last *ca.* 3 million years, which may have connected today's disjunct species ranges in the western part of the HTO, for example *Chrysopaa sternosignata*, *Nanorana hazarensis*, *N. vicina*, with the projected suitable habitats (and/or the potential area of origin) at the opposite side of the orogenic system; and (iii) the (large-scale) areas of suitable habitats across central and Southeast China, particularly for *N. hazarensis*, and *N. vicina*, are far outside their native distribution in the West Himalaya. Although MESS-maps indicate that large areas across the modelled extension are associated with uncertainty, phylogenetic niche modelling yielded similar results, arguing against in situ speciation.

### 3.3 | Ancestral range and divergence time estimation in spiny frogs of the HTO

The best-fitting ARE model under the constraints of the paleoenvironmental scenario of Schmidt et al. (2023) was DIVALIKE, showing an extinction rate ('e') of 0.039 events/Myr, and an anagenetic dispersal rate ('d') of 0.055 events/Myr. The parameters and likelihoods of the three models assessed are summarized in Table S6.

The crown age of spiny frogs from the HTO is estimated to be ca. 29.7 (20.9–38.7) Ma (Figures 5 and S10), and their separation from other lineages of the Dicroglossidae group occurred at ca. 65.1 (55.0–75.8) Ma (Figures S11 and S12). The ancestors of *Nanorana* and *Quasipaa*/*Chrysopaa* probably originated from Southeast Asia and/or the adjacent southwestern Hengduan Shan (area combination AJ; Figures 5, S13 and S14). From Southeast Asia, the ancestral lineage of the subtropical *Chrysopaa* had spread northwards probably through the Kunlun Shan (area O) to reach the far western Hindukush (area Z; *Chrysopaa*), while *Quasipaa* diversified in tropical areas across Southeast Asia, and southern-central and eastern China; both genera diverged ca. 18.0 (9.4–27.8) Ma.

The ancestral lineages of the temperate and (sub)alpine group (*Chaparana*/*Allopaa*, *Nanorana*, *Paa*) were separated from the (sub) tropical lineages by vicariance and spread from regions of the southwestern Hengduan Shan into the Gangdese Shan (area combination JG). The Himalayan spiny frogs (*Paa*) split again by vicariance from the *Chaparana*/*Allopaa* and the (sub)alpine *Nanorana* lineages during the very Early Miocene ca. 21.5 (14.8–29.4) Ma and had their ancestral range probably in the Gangdese Shan. Ancestors of the cold-adapted *Nanorana* dispersed from the southwestern Hengduan Shan into northern, (sub)alpine areas of the Hengduan Mountains (area H; combination HJ) and later back into the Gangdese Shan (*N. parkeri*); they separated from the warm temperate *Chaparana*/*Allopaa* ca. 20.0 (13.1–27.1) Ma (according to the topology m1), or ca. 19.7 (12.4–27.7) Ma (based on topology m0) from the temperate *Paa* and *N. minica* (Figure S12). Ancestral lineages of *Chaparana*/*Allopaa*, on the other hand, spread throughout the Hengduan Shan and further west into the Qiangtang, with *Allopaa hazarensis* diverging from *Chaparana* ca. 18.0 (11.3–24.7) Ma (i.e. about the same time when *Chrysopaa* split from *Quasipaa*); *Allopaa* probably dispersed through the Qiangtang to enter the West Himalaya.

The ancestor of the subgenus *Paa* dispersed from the Gangdese Shan into the West Himalaya and separated ca. 19.0 (11.9–26.6) Ma. Later, *Nanorana* (*Paa*) *vicina* also originated by vicariance of the Gangdese Shan and the West Himalaya ca. 8.2 (5.3–11.5 Ma). Other ancestral *Paa* lineages moved from the Gangdese Shan into the Central Himalaya (area C; combination GC), where they also separated by vicariance ca. 7.3 (4.8–10.2) Ma from those lineages that dispersed from the Gangdese Shan into the East Himalaya (area E). From the East Himalaya some lineages (*N. medogensis*, *N. maculosa* and *N. chayuensis*) dispersed back into the adjacent southwestern Hengudan Shan and separated by vicariance ca. 3.4–2.2 Ma.

Notably, all deeper splits (≥18.0 Ma) match the period during which humid, (warm-)temperate areas may have existed in Paleo-South Tibet according to the paleoenvironmental scenario of Schmidt et al. (2023) (Figures 5 and S10).

Diversification of Himalayan spiny frogs, except the West-Himalayan *Nanorana* (*Paa*) *minica*, occurred continuously during the entire Late Cenozoic, starting in the Late Miocene ca. 8 Ma. All main lineages within this group were present ~5–7 Ma, and all species are older than the Pliocene-Pleistocene boundary.

Range shifts and range expansions were the dominant events in the evolutionary history of spiny frogs, whereas vicariance was less important, as shown by BSM (Figure S15). Narrow sympatry

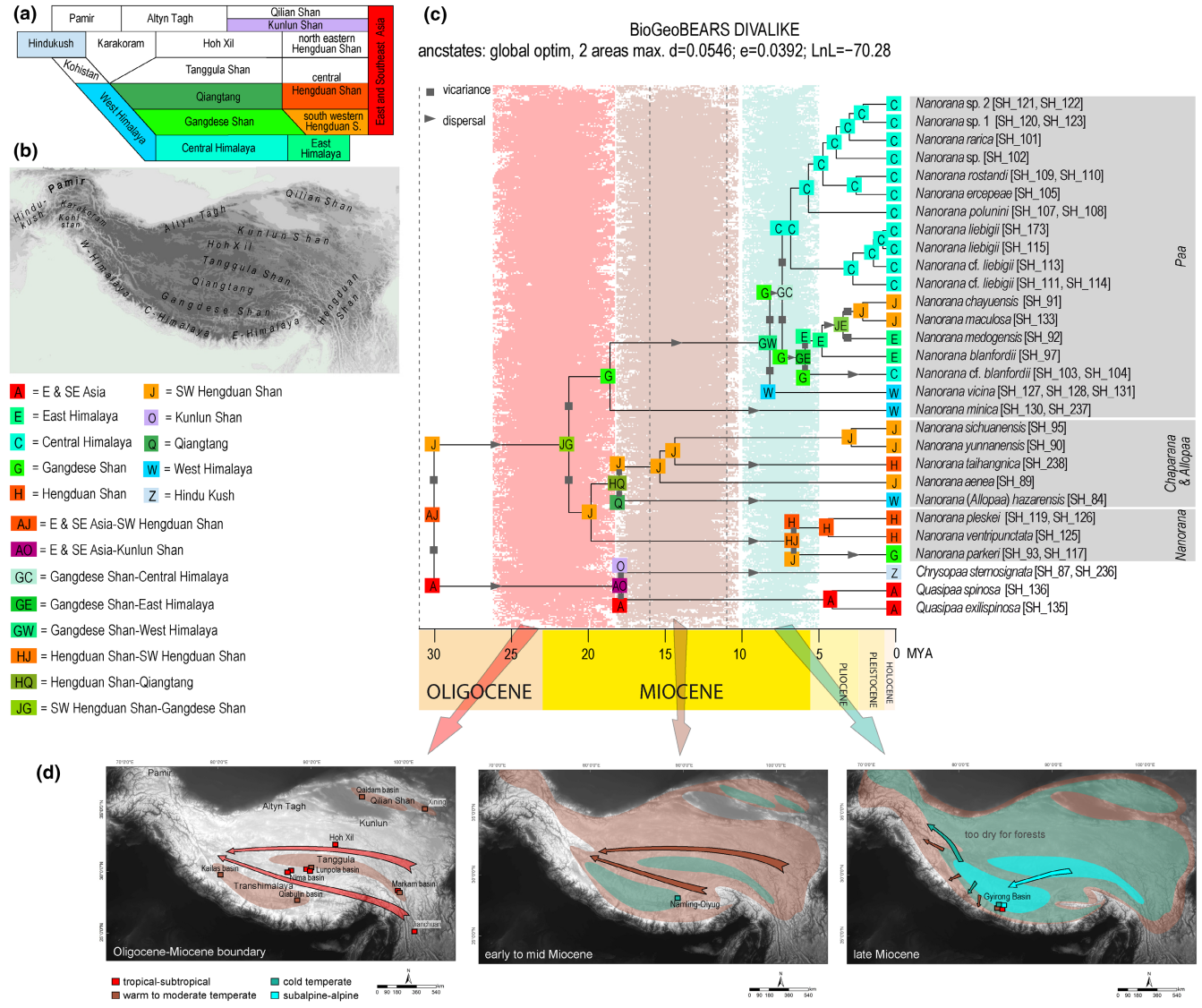


FIGURE 5 Divergence times and paleobiogeography of spiny frogs across the HTO. (a) Schematic map of the 19 areas as coded for BioGeoBEARS, and (b) plotted to the HTO grid layer. (c) Chronogram derived from the BEAST2 analysis presenting the median ages estimated. (d) Modified illustration of the Oligocene-Miocene paleoenvironmental evolution of the HTO according to Schmidt et al. (2023). Proposed extensions of temperate and alpine environments are shown as coloured areas; coloured arrows indicate the movement of spiny frogs across paleo-Tibet; coloured squares represent paleontological records (for details, see Table S2 in Schmidt et al., 2023). Only the most likely ancestral ranges as estimated under the DIVALIKE model in BioGeoBEARS are coloured in (a), (b), and presented in the colour legend. Mya, millions of years ago.

(i.e. cladogenetic event within one area) also played a prominent role in the evolution of this group. The state probabilities of the BSM were strongly congruent with those of the ML approach (Figure S16).

## 4 | DISCUSSION

In this study, we provide the first genomic data-based, time-calibrated phylogeny of spiny frogs distributed across the HTO, as well as biogeographic and niche models to reconstruct the evolutionary history of that group against the background of a recent paleoenvironmental scenario for the HTO (Schmidt et al., 2023).

### 4.1 | Caveats of the study

Some potential methodological issues may have impacted our results, although they most likely should not overturn our major conclusions. First, our niche modelling approach suffers from the lack of fossil occurrence data to validate model transferability and ancestral reconstructions. Fossil records are the only positive source of information to unambiguously detect shifts in the distribution of suitable habitat due to changes in climate regime or tectonic activity. Unfortunately, anuran fossils are generally rare across the HTO; so far, only a few Ranidae records are known from the Siwalik belt of Jammu province, India, dating to the Upper Pliocene (Rage et al., 2016).

Moreover, the PaleoClim simulations are based on a global topography that is largely similar to the modern topography. Thus, potential topographic changes across the HTO over the last 3 million years that may have impacted local climate are not considered. High-resolution paleo-DEMs that are informed by a global plate-model and detailed paleogeographic reconstructions may exist (e.g. at deeptimemaps.com, and Getech Group, see Chiarenza et al., 2019), but they are not publicly accessible. More global topographic and paleoclimate circulation models are urgently needed to describe distributions of climate through deep time and to help interpreting the geographic distribution of ancient climate availability. Currently, estimating geographical ranges of the past appears still limited.

We also acknowledge that our sampling of spiny frog clades is not comprehensive. In particular, we lack species that have been described very recently from the eastern margin of the HTO and/or are only known from their type locality (e.g. *Nanorana bangdaensis*, *N. feae*, *N. kangxianensis*, *N. xuelinensis* and *N. zhaoermii*). Despite these limitations, we have included all known major clades of spiny frogs of the HTO.

## 4.2 | Indications for thermal niche conservatism and geographic range shifts

Most amphibians have relatively narrow climatic niche widths, especially with respect to temperature and precipitation, and their rate of niche evolution is rather slow (Bonetti & Wiens, 2014; Quintero & Wiens, 2013). Under environmental changes accompanied by mountain building, species with narrow niche space are those whose geographical ranges are then most likely to move outside their climatic niche.

The topographic evolution of the HTO with the building of high-altitude mountain ranges has actively forced climatic change (An et al., 2001; Boos & Kuang, 2010; Kutzbach et al., 1993; Molnar et al., 1993). Spiny frogs could respond to these large-scale transitions in environmental regimes in two non-exclusive ways: (i) adapting their climatic niche to fit the new conditions or (ii) changing their geographic range to track the conditions that are compatible with their climatic niche (Bonetti & Wiens, 2014; Visser, 2008); or (failing these two options), go extinct.

Both our results, the environmental niche profiles (represented by bio1 and bio12), and ancestral state estimation of temperature and precipitation (Figure 3), indicate a significant level of niche conservatism, that is the tendency for members of a clade to maintain ancestral ecological niche characteristics over time, which has been linked to allopatric speciation (Wiens et al., 2010; Wiens & Donoghue, 2004; Wiens & Graham, 2005). This is also backed by the significant phylogenetic signal in both, the mean annual temperature and precipitation recovered from the calibrated tree. Ecological correlations, particularly those concerning distinct spiny frog clades, suggest that the considerable physiological adaptations necessary for transitioning between different climatic niches in response to the dramatic environmental changes in the HTO may not be as readily achievable as anticipated under a scenario dominated by in situ speciation (Donoghue, 2008). It has been demonstrated that transitions between tropical and temperate habitats in amphibians are often limited due to niche conservatism (Pyron & Wiens, 2013; Wiens et al., 2006). This observed pattern may or may not contribute to the relatively small number of cold-adapted taxa observed in *Nanorana* spiny frogs. Specifically, only a single group of these frogs, the nominal subgenus *Nanorana*, appears to have successfully transitioned to alpine, highly seasonal environments. It is hypothesized that this transition occurred from an ancestrally temperate lineage (Figure 3). However, this interpretation must be treated with caution, as there are limited comparisons available for how adaptable these frogs are versus other groups. Notably, we assume that the lack of suitable outgroups and large proportion of temperate taxa in the calibrated tree may have biased our ancestral state estimation towards reconstructing lower ancestral temperature patterns, which we suspect were probably more (sub)tropical (Figure 3c), also in view of the suggested origin of spiny frogs in tropical Southeast Asia (Che et al., 2010; Hofmann et al., 2019). Our indications of niche conservatism in spiny frogs are consistent with results obtained in *Gynandropaa* clades (all moved into the genus *Nanorana* (Frost, 2024): *N. yunnanensis*, *N. sichuanensis* and *N. phrynoides*), which suggest a common ancestral ecological niche of that group and divergence through allopatric speciation (Hu et al., 2016).

Our projections illustrate the potentially highly dynamic ranges of spiny frogs in the HTO in response to climate changes over the past 3 million years. Range shifts and niche stability have frequently been observed in amphibians, including *Nanorana*, although mostly over shorter geological time scales (Araújo et al., 2008; Wang et al., 2017; Zhou et al., 2014). Notably, projecting the climatic niche of species to past periods is not projecting the distribution of species (Nogués-Bravo, 2009). For example, the (remarkably large) projected areas of high habitat suitability in East and Southeast China for *Nanorana* (*Allopaa*) *hazarensis* and *N.* (*Paa*) *vicina* do not coincide with sites where the species are present. If their ancestral lineages ever occupied the entirety of that eastern area, they must have been extirpated—a scenario that is implausible given the recent distribution of *Chaparana* and *Quasipaa* species in Southeast China, some of which share a similar environmental niche with the two taxa from the West Himalaya. We instead assume that the ancestral lineages of today's West-Himalayan clades occurred in regions of southern-central Tibet, for example in the paleo-Gangdese Shan and/or paleo-Tanggula Shan and were separated from closely related clades in East and Southeast Asia during the Late Cenozoic uplift of the HTO. From there, ancestors may have been forced to follow their climate niches to the West when primary distribution ranges were lost due to the cooling and aridification of Tibet (see further Discussion below). Species with such highly dynamic paleogeographic ranges are expected to have very low genetic diversity and small geographic ranges today, due to the climate-driven geographic bottlenecks experienced in the past (Rödder et al., 2013). Indeed, the genetic diversity of *Nanorana* (*Allopaa*) *hazarensis* across its known range is low

and without a clear distribution pattern of haplotypes (Hofmann, Jablonski, et al., 2021). We suspect that low levels of genetic structure may also be present within *Chrysopaa* (Hofmann et al., 2023) and *N.* (*Paa*) *minica*, and perhaps *N.* (*Paa*) *vicina*.

Overall, our modelling results indicate that range shifts in response to environmental changes may have been common in spiny frogs (Figures 4 and S8a–d). We assume that it might have been easier for spiny frogs to follow their habitat to which they had adapted and move into suitable regions in response to uplift and corresponding climatic change in vast areas, instead of adapting to the new conditions. Given recent models on the evolution of the HTO and fossil findings (see below), suitable corridors might have existed during the Miocene (and even earlier) that may have promoted the migration of species across paleo-Tibet.

### 4.3 | Paleobiogeography of spiny frogs in warm temperate Miocene Tibet

Our recovered topologies and divergence times (Figures 1 and 5) agree largely with prior hypotheses of Himalayan spiny frog relationships and clade ages based on a few genetic loci (Che et al., 2010; Hofmann et al., 2019, 2023; Hofmann, Jablonski, et al., 2021) or taxa (Sun et al., 2018) (Table S7), with three notable exceptions: the placement of the genus *Chrysopaa*, the nominal subgenus *Nanorana*, and the species *N. minica*. Here, we resolve *Chrysopaa* as sister to *Quasipaa* in all analyses, resulting in a younger separation time between both (18 Ma) compared with previous estimations (~26–28 Ma; Hofmann, Jablonski, et al., 2021; Hofmann et al., 2023). Noteworthy, the most recent large-scale frog phylogeny, based on a gigamatrix approach, could not reveal this genus-level sister relationship, probably because of extensive missing genomic data for those taxa (Portik et al., 2023). The (sub)alpine, nominal subgenus *Nanorana* separated ca. 20 Ma, either from *Chaparana* + *Allopaa*, or from *Paa*; this is consistent with the estimation by Che et al. (2010), but older than our previous results (9–15 Ma). The West-Himalayan *N. minica* separated from all remaining Himalayan spiny frogs (subgenus *Paa*) ca. 17–19 Ma, similar to our previous estimation (Hofmann et al., 2023).

The crown age of spiny frogs at about 30 Ma indicates the earliest possible existence of a common ancestral area. Under the constraints of the paleoenvironmental scenario of Schmidt et al. (2023), their common ancestor probably had a tropical distribution in the southwestern Hengduan Shan and East/Southeast Asia (Figure 5), confirming previous suggestions (Che et al., 2010; Hofmann et al., 2019). We assume that from this time on, the emergence of habitats, for example along the current Gangdese Shan, suitable for *Nanorana* species that were pre-adapted to temperate climates triggered their separation from (sub)tropical lineages. Almost the same age (29 Ma) has been observed in the forest-dwelling amphibian genus *Scutiger* of the HTO (Hofmann et al., 2017), and a slightly younger age (ca. 27 Ma) has been shown for the ancient Himalayan ground beetles *Carabus* and *Pterostichus* (Schmidt et al., 2012, 2023).

The subsequent separation of Himalayan spiny frogs (subgenus *Paa*), with a potential ancestral range across the Gangdese Shan (Figure 5), from lineages at the eastern margin of Tibet (subgenera *Allopaa*, *Chaparana* and *Nanorana*) during the Early Miocene (~22 Ma) was probably linked to a significant climatic change resulting from uplift of certain parts of the HTO, isolating the Gangdese from the southwestern Hengduan Shan. The split of the ancestral cold-adapted *Nanorana* from the montane subtropical/warm temperate *Chaparana* ca. 20 Ma indicates further range shifts or, alternatively, uplift in the regions of today's central and northern Hengduan Shan. However, the crown age of this (sub)alpine *Nanorana* clade is relatively young (Figures 5 and S10; Che et al., 2010; Hofmann et al., 2019, 2023; Hofmann, Jablonski, et al., 2021), indicating the emergence of high-altitude habitats not before the very late Miocene or Miocene–Pliocene boundary. This contrasts with models derived from stable isotope paleoaltimetry that propose large-scale alpine environments across paleo-Tibet since the Late Eocene or even earlier (Kapp et al., 2007; Murphy et al., 1997; Tapponnier et al., 2001; Wang et al., 2008, 2014).

Most notably, three lineages, namely *Nanorana minica* and *N. hazarensis* from the western Himalaya, and *Chrysopaa* from the Hindukush, diverged from their respective ancestor at almost the same time during the Mid-Miocene (~18–19 Ma; Figure 5). All three taxa occur in montane, warm temperate or subtropical habitats at elevations between 1000 m and ~2000 m (*N. hazarensis*) or up to ~2500 m (*Chrysopaa*, *N. minica*) (Frost, 2024; Hofmann et al., 2023). The respective closest relatives of *N. hazarensis* and *Chrysopaa*, namely representatives of the warm temperate or subtropical *Chaparana* and tropical *Quasipaa*, occur on the opposite side of the HTO; in *N. minica*, the central and eastern Himalayan *Paa* are closest. We suspect that these Mid-Miocene simultaneous divergence events point to the successive disappearance of formerly continuous areas that facilitated an east–west trans-Tibetan distribution of ancestral lineages of these spiny frogs due to surface uplift in Tibet's interior and related cooling and drying. According to our biogeographic model (Figure 5) and fossil findings (see below), potential low-elevation, warm temperate or (sub)tropical corridors across paleo-Tibet may have existed during the Early Miocene along the Kunlun Shan, Qiangtang and/or Gangdese Shan.

The evolution of the Himalayan spiny frogs of the subgenus *Paa* provides spatio-temporal information on the uplift of mountains on the southern margin of the HTO. Under the paleoenvironmental scenario of Schmidt et al. (2023) and our model findings, these taxa began to diversify in paleo-South Tibet during the lower Miocene, suggesting a significant surface uplift and associated cooling of the environment. We assume that the ancestral fauna of paleo-South Tibet might have been forced to track their ecological niches along the Himalayan transverse valleys towards the HTO margins into suitable, (cold) temperate habitats of the growing Himalaya (Schmidt et al., 2012), in response to uplift-driven climate changes. The lineages were further isolated by vicariance during the rising Himalayas, as indicated by extensive geographically structured relationships among the West, Central

and East Himalayan clades. We observed very similar results in the Himalayan lazy toads (*Scutiger*) (Hofmann et al., 2017).

The most supportive data for our scenario comes from fossil evidence: tropical to warm temperate fossil floras have been found in the Lunpola and Qiabulin basins in central-southern Tibet, and dated to the Oligocene-Miocene boundary/late early Miocene (e.g. Ding et al., 2017; Sun et al., 2014; Wu et al., 2017), whereas the Namling flora points to the existence of temperate forests in the central Gangdese Shan during the Mid-Miocene (ca. 15 Ma; Spicer et al., 2003; Zhou et al., 2007). Also noteworthy are geochemical marine signatures in the Qaidam basin (between the Altyn Thag and Kunlun Shan; Figure 5), indicating uplift to the present basin altitude, ca. 3000 m, not before the Mid-Miocene (Sun et al., 2023). Thus, the existence of east–west orientated (warm) temperate areas by the Early Miocene has been suggested, potentially acting as 'niche corridor' for Asian biodiversity (Schmidt et al., 2023; Spicer et al., 2021b).

## 5 | CONCLUSIONS

From the large number of existing phylogenetic studies on species groups of the HTO, it becomes clear that previous models of the HTO uplift cannot adequately explain the pattern and evolution of faunal biodiversity across this orogenic system (Renner, 2016). Renner (l.c.) suggested that inconsistencies between phylogenetic insights and geological models result from insufficient consideration of recent findings in tectonics, isotope physics, palaeontology and climate modelling when interpreting phylogeographic data. There is still a need for alternative scenarios of the evolution of the HTO that may explain the historical biogeography of its biota.

The present phylogeographic pattern of spiny frogs also cannot be reasonably explained by modern geoscientific scenarios assuming a paleo-Tibet with near-present elevation, that supposedly existed as early as the Late Eocene. We, instead, found strong indications for trans-Tibet movements of thermophilic species at least until the Early Miocene, which can be fully explained by a (sub) tropical to (warm-)temperate paleoclimate of Miocene Tibet, as previously postulated (Schmidt et al., 2023) and supported by fossil records (see Discussion above). Moreover, our data show that spiny frogs, although present in the HTO area since the Oligocene period, did not adapt to the cold temperate and subalpine environments before the Late Miocene. These results are consistent with the hypothesis of a young age of the alpine environment in the HTO, at ca. the Miocene/Pliocene boundary (Hofmann et al., 2017, 2019; Schmidt et al., 2023). Assuming areas with lower elevation across South Tibet during the Miocene, which were accompanied by a warm paleoenvironment, we suggest that the modern disjunct distributions of spiny frogs might be largely a result of their westwards and southwards retreat as suitable climates across paleo-Tibet receded in the Oligocene and Miocene due to ongoing orogenesis. We conclude that the spiny frogs maintained their (sub)tropical or (warm) temperate physiological tolerances and moved out of the ancestral paleo-Tibetan area, probably along Himalayan epigenetic transverse valleys, towards the west and to the south into the 'Himalayan exile' (Schmidt et al., 2012) as the climate shifted, as opposed to adapting to the alpine in situ. Although we are aware of potential caveats of our study (see Supplementary Information Text), we expect that the phylogenies of other ectothermic groups endemic to the HTO with low dispersal capacity and similar ecological attributes might reflect processes and biogeographic patterns similar to those shown here for spiny frogs and previously shown for lazy toads (Hofmann et al., 2017) and ground beetles (Schmidt et al., 2012). We assume that the high levels of richness and endemicity observed in numerous species on Himalayan mountains likely bear the signatures of deep-time evolutionary and ecological processes, driven by changing climate across topographically complex landscapes and by biotic interchange with adjacent areas (Rahbek et al., 2019). In a broader context, our study enhances comprehension of mountain formation processes and the interplay between biodiversity and geology.

### AUTHOR CONTRIBUTIONS

*Conceptualization*: Sylvia Hofmann, Joachim Schmidt, and Lars Podsiadlowski. *Methodology*: Sylvia Hofmann, Dennis Rödder,Lars Podsiadlowski, Michael Matschiner, Michael Nothnagel, Sebastian Martin, and Tobias Andermann. *Investigation*: Sylvia Hofmann. *Analysis*: Sylvia Hofmann, Dennis Rödder, Michael Matschiner, and Lars Podsiadlowski. *Visualization*: Sylvia Hofmann, Dennis Rödder, and Morris Flecks. *Supervision*; *writing—original draft*: Sylvia Hofmann. *Resources*: Sylvia Hofmann, Michael Matschiner, Chitra B. Baniya, Jianhuan Yang, Ke Jiang, Jiang Jianping, Spartak N. Litvinchuk, Rafaqat Masroor, Michael Nothnagel, Vladimir Vershinin, Yuchi Zheng, Daniel Jablonski, Joachim Schmidt, Lars Podsiadlowski. *Writing—review and editing*: all authors.

### ACKNOWLEDGEMENTS

We thank four anonymous reviewers for their valuable input that helped to improve the manuscript. We are also very grateful to Sandra Kukowka (LIB, Museum Koenig) for skilled laboratory work, to Benedikt Wystup (Bechtle GmbH & Co) for IT assistance and support, Edi Stoeckli (Natural History Museum Basel) for helping with the museum material, and to Matthias Hartmann and Konrad Kürbis (NHME), Gunther Köhler (SMF), Jia-Tang Li (CAS), and Mark-Oliver Rödel (ZMB) for providing samples. Computations were performed on resources provided by Sigma2—the National Infrastructure for High-Performance Computing and Data Storage in Norway, at the High-Performance Computing (HPC) system of the Museum Koenig Bonn, and on the DFG-funded HPC system, CHEOPS at the Regional Computing Center of the University of Cologne.

### FUNDING INFORMATION

The project was funded by the German Research Foundation (DFG) (grant number: HO 3792/8-1 to SH). The work was also supported

within the frameworks of state contract No. 122021000082-0 with the Institute of Plant and Animal Ecology, Ural Branch, Russian Academy of Sciences.

## CONFLICT OF INTEREST STATEMENT

The authors have no conflicts of interest to declare that are relevant to the content of this manuscript.

## DATA AVAILABILITY STATEMENT

Raw sequence reads have been deposited in the NCBI Sequence Read Archive under BioProject PRJNA1025371. Phylogenetic trees, records and maps of SDM and PNM can be accessed at figshare repository: https://doi.org/10.6084/m9.figshare.24306367.

## ORCID

*Sylvia Hofmann* https://orcid.org/0000-0003-0621-9049
*Dennis Rödder* https://orcid.org/0000-0002-6108-1639
*Tobias Andermann* https://orcid.org/0000-0002-0932-1623
*Michael Matschiner* https://orcid.org/0000-0003-4741-3884
*Jiang Jianping* https://orcid.org/0000-0002-1051-7797
*Yuchi Zheng* https://orcid.org/0000-0002-1155-5293

## REFERENCES

Aberer, A. J., Kobert, K., & Stamatakis, A. (2014). ExaBayes: Massively parallel bayesian tree inference for the whole-genome era. *Molecular Biology and Evolution*, *31*, 2553–2556.

Ai, K., Shi, G., Zhang, K., Ji, J., Song, B., Shen, T., & Guo, S. (2019). The uppermost Oligocene Kailas flora from southern Tibetan Plateau and its implications for the uplift history of the southern Lhasa terrane. *Palaeogeography, Palaeoclimatology, Palaeoecology*, *515*, 143–151.

An, Z. S., Kutzbach, J. E., Prell, W. L., & Porter, S. C. (2001). Evolution of Asian monsoons and phased uplift of the Himalaya-Tibetan Plateau since late Miocene times. *Nature*, *411*, 62–66.

Araújo, M. B., Nogués-Bravo, D., Diniz-Filho, J. A. F., Haywood, A. M., Valdes, P. J., & Rahbek, C. (2008). Quaternary climate changes explain diversity among reptiles and amphibians. *Ecography*, *31*, 8–15.

Atkinson, T. C., Briffa, K. R., & Coope, G. R. (1987). Seasonal temperatures in Britain during the past 22,000 years, reconstructed using beetle remains. *Nature*, *325*, 587–592.

Beebee, T. J. C. (1995). Amphibian breeding and climate. *Nature*, *374*, 219–220.

Bi, K., Vanderpool, D., Singhal, S., Linderoth, T., Moritz, C., & Good, J. M. (2012). Transcriptome-based exon capture enables highly cost-effective comparative genomic data collection at moderate evolutionary scales. *BMC Genomics*, *13*, 403.

Blackburn, D. C., Roberts, E. M., & Stevens, N. J. (2015). The earliest record of the endemic African frog family Ptychadenidae from the Oligocene Nsungwe formation of Tanzania. *Journal of Vertebrate Paleontology*, *35*, e907174.

Blomberg, S. P., Garland, T., Jr., & Ives, A. R. (2003). Testing for phylogenetic signal in comparative data: Behavioral traits are more labile. *Evolution*, *57*, 717–745.

Bonetti, M. F., & Wiens, J. J. (2014). Evolution of climatic niche specialization: A phylogenetic analysis in amphibians. *Proceedings of the Biological Sciences*, *281*, 20133229.

Boos, W. R., & Kuang, Z. M. (2010). Dominant control of the south Asian monsoon by orographic insulation versus plateau heating. *Nature*, *463*, 218–222.

Bossuyt, F., Brown, R. M., Hillis, D. M., Cannatella, D. C., & Milinkovitch, M. C. (2006). Phylogeny and biogeography of a cosmopolitan frog radiation: Late cretaceous diversification resulted in continent-scale endemism in the family ranidae. *Systematic Biology*, *55*, 579–594.

Bouckaert, R., Vaughan, T. G., Barido-Sottani, J., Duchêne, S., Fourment, M., Gavryushkina, A., Heled, J., Jones, G., Kühnert, D., de Maio, N., Matschiner, M., Mendes, F. K., Müller, N. F., Ogilvie, H. A., du Plessis, L., Popinga, A., Rambaut, A., Rasmussen, D., Siveroni, I., … Drummond, A. J. (2019). BEAST 2.5: An advanced software platform for Bayesian evolutionary analysis. *PLoS Computational Biology*, *15*, e1006650.

Brown, J. L., Hill, D. J., Dolan, A. M., Carnaval, A. C., & Haywood, A. M. (2018). PaleoClim, high spatial resolution paleoclimate surfaces for global land areas. *Scientific Data*, *5*, 180254.

Brühl, C. (1997). Flightless insects: A test case for historical relationships of African mountains. *Journal of Biogeography*, *24*, 233–250.

Che, J., Zhou, W. W., Hu, J. S., Yan, F., Papenfuss, T. J., Wake, D. B., & Zhang, Y. P. (2010). Spiny frogs (Paini) illuminate the history of the Himalayan region and Southeast Asia. *Proceedings of the National Academy of Sciences of the United States of America*, *107*, 13765–13770.

Chiarenza, A. A., Mannion, P. D., Lunt, D. J., Farnsworth, A., Jones, L. A., Kelland, S. J., & Allison, P. A. (2019). Ecological niche modelling does not support climatically-driven dinosaur diversity decline before the Cretaceous/Paleogene mass extinction. *Nature Communications*, *10*, 1091.

Coleman, M., & Hodges, K. (1995). Evidence for Tibetan Plateau uplift before 14Myr ago from a new minimum estimate for east–west extension. *Nature*, *374*, 49–52.

Criscuolo, A., & Gribaldo, S. (2010). BMGE (block mapping and gathering with entropy): A new software for selection of phylogenetic informative regions from multiple sequence alignments. *BMC Evolutionary Biology*, *10*, 210.

Cruz, J. A., Basanta, M. D., García-Castillo, M. G., Wooldrich-Piña, G. A., & Parra-Olea, G. (2024). Amphibians environmental dependence and their use in Paleoecological reconstructions. In R. Guerrero-Arenas & E. Jiménez-Hidalgo (Eds.), *Past environments of Mexico* (pp. 253–271). Springer.

Deng, T., Wang, X., Wu, F., Wang, Y., Li, Q., Wang, S., & Hou, S. (2019). Review: Implications of vertebrate fossils for paleo-elevations of the Tibetan Plateau. *Global and Planetary Change*, *174*, 58–69.

Ding, L., Spicer, R. A., Yang, J., Xu, Q., Cai, F., Li, S., Lai, Q., Wang, H., Spicer, T. E. V., Yue, Y., Shukla, A., Srivastava, G., Khan, M. A., Bera, S., & Mehrotra, R. (2017). Quantifying the rise of the Himalaya orogen and implications for the south Asian monsoon. *Geology*, *45*, 215–218.

Ding, L., Xu, Q., Yue, Y., Wang, H., Cai, F., & Li, S. (2014). The Andean-type Gangdese Mountains: Paleoelevation record from the Paleocene–Eocene Linzhou Basin. *Earth and Planetary Science Letters*, *392*, 250–264.

Dolan, A. M., Haywood, A. M., Hunter, S. J., Tindall, J. C., Dowsett, H. J., Hill, D. J., & Pickering, S. J. (2015). Modelling the enigmatic Late Pliocene Glacial Event—Marine Isotope Stage M2. *Global and Planetary Change*, *128*, 47–60.

Donoghue, M. J. (2008). Colloquium paper: A phylogenetic perspective on the distribution of plant diversity. *Proceedings of the National Academy of Sciences of the United States of America*, *105 Suppl 1*, 11549–11555.

Drummond, A. J., & Rambaut, A. (2007). BEAST: Bayesian evolutionary analysis by sampling trees. *BMC Evolutionary Biology*, *7*, 214.

Dupin, J., Matzke, N., Sarkinen, T., Knapp, S., Olmstead, R. G., Bohs, L., & Smith, S. D. (2016). Bayesian estimation of the global biogeographic history of the Solanaceae. *Journal of Biogeography*, *44*, 887–899.

Elith, J., Kearney, M., & Phillips, S. J. (2010). The art of modelling range-shifting species. *Methods in Ecology and Evolution*, *1*, 330–342.

Evans, M. E., Smith, S. A., Flynn, R. S., & Donoghue, M. J. (2009). Climate, niche evolution, and diversification of the "bird-cage" evening primroses (Oenothera, sections Anogra and Kleinia). *The American Naturalist*, *173*, 225–240.

Fang, X., Dupont-Nivet, G., Wang, C., Song, C., Meng, Q., Zhang, W., Nie, J., Zhang, T., Mao, Z., & Chen, Y. (2020). Revised chronology of central Tibet uplift (Lunpola Basin). *Science Advances*, *6*, eaba7298.

Freckleton, R. P., Harvey, P. H., & Pagel, M. (2002). Phylogenetic analysis and comparative data: A test and review of evidence. *The American Naturalist*, *160*, 712–726.

Frost, D. R. (2024). *Amphibian species of the world: an online reference. Version 6.2. Electronic Database accessible at https://amphibiansoftheworld.amnh.org/index.php*. American Museum of Natural History. http://research.amnh.org/herpetology/amphibia/index.html

Ginal, P., Tan, W. C., & Rödder, D. (2022). Invasive risk assessment and expansion of the realized niche of the *Calotes versicolor* species complex (Daudin, 1802). *Frontiers of Biogeography*, *14*(3), e54299.

Girgis, H. Z. (2022). MeShClust v3.0: High-quality clustering of DNA sequences using the mean shift algorithm and alignment-free identity scores. *BMC Genomics*, *23*, 423.

Guillory, W. X., & Brown, J. L. (2021). A new method for integrating ecological Niche modeling with Phylogenetics to estimate ancestral distributions. *Systematic Biology*, *70*, 1033–1045.

Guindon, S., Dufayard, J. F., Lefort, V., Anisimova, M., Hordijk, W., & Gascuel, O. (2010). New algorithms and methods to estimate maximum-likelihood phylogenies: Assessing the performance of PhyML 3.0. *Systematic Biology*, *59*, 307–321.

Harrison, T. M., Copeland, P., Kidd, W. S., & Yin, A. (1992). Raising Tibet. *Science*, *255*, 1663–1670.

Hedges, S. B., Marin, J., Suleski, M., Paymer, M., & Kumar, S. (2015). Tree of life reveals clock-like speciation and diversification. *Molecular Biology and Evolution*, *32*, 835–845.

Heibl, C., & Calenge, C. (2018). phyloclim: Integrating Phylogenetics and climatic niche modeling. R package version 0.9.5.

Hill, D. J. (2015). The non-analogue nature of Pliocene temperature gradients. *Earth and Planetary Science Letters*, *425*, 232–241.

Hofmann, S., Baniya, C. B., Litvinchuk, S. N., Miehe, G., Li, J. T., & Schmidt, J. (2019). Phylogeny of spiny frogs *Nanorana* (Anura: Dicroglossidae) supports a Tibetan origin of a Himalayan species group. *Ecology and Evolution*, *9*, 14498–14511.

Hofmann, S., Jablonski, D., Litvinchuk, S. N., Masroor, R., & Schmidt, J. (2021). Relict groups of spiny frogs indicate Late Paleogene-early Neogene trans-Tibet dispersal of thermophile faunal elements. *PeerJ*, *9*, e11793.

Hofmann, S., Masroor, R., & Jablonski, D. (2021). Morphological and molecular data on tadpoles of the westernmost Himalayan spiny frog *Allopaa hazarensis* (Dubois and Khan, 1979). *ZooKeys*, *1049*, 67–77.

Hofmann, S., Schmidt, J. L., Masroor, R., Borkin, L. J., Litvintchuk, S., Rödder, D., Vershinin, V., & Jablonski, D. (2023). Endemic lineages of spiny frogs demonstrate the biogeographic importance and conservational needs of the Hindu Kush–Himalaya region. *Zoological Journal of the Linnean Society*, *198*, 310–325.

Hofmann, S., Stoeck, M., Zheng, Y., Ficetola, F. G., Li, J.-T., Scheidt, U., & Schmidt, J. (2017). Molecular phylogenies indicate a Paleo-Tibetan origin of Himalayan lazy toads (*Scutiger*). *Scientific Reports*, *7*, 3308.

Höhna, S., Heath, T. A., Boussau, B., Landis, M. J., Ronquist, F., & Huelsenbeck, J. P. (2014). Probabilistic graphical model representation in phylogenetics. *Systematic Biology*, *63*, 753–771.

Höhna, S., Landis, M. J., Heath, T. A., Boussau, B., Lartillot, N., Moore, B. R., Huelsenbeck, J. P., & Ronquist, F. (2016). RevBayes: Bayesian phylogenetic inference using graphical models and an interactive model-specification language. *Systematic Biology*, *65*, 726–736.

Hoorn, C., Mosbrugger, V., Mulch, A., & Antonelli, A. (2013). Biodiversity from mountain building. *Nature Geoscience*, *6*, 154.

Hu, J., Broennimann, O., Guisan, A., Wang, B., Huang, Y., & Jiang, J. (2016). Niche conservatism in Gynandropaa frogs on the southeastern Qinghai-Tibetan Plateau. *Scientific Reports*, *6*, 32624.

Hutter, C. R., Guayasamin, J. M., & Wiens, J. J. (2013). Explaining Andean megadiversity: The evolutionary and ecological causes of glassfrog elevational richness patterns. *Ecology Letters*, *16*, 1135–1144.

Kapp, P., DeCelles, P. G., Leier, A. L., Fabijanic, J. M., He, S., Pullen, A., Gehrels, G. E., & Ding, L. (2007). The Gangdese retroarc thrust belt revealed. *GSA Today*, *17*, 4–9.

Karger, D. N., Conrad, O., Böhner, J., Kawohl, T., Kreft, H., Soria-Auza, R. W., Zimmermann, N. E., Peter Linder, H., & Kessler, M. (2018). Climatologies at high resolution for the earth's land surface areas. Dryad Digital Repository.

Katoh, K., & Standley, D. M. (2013). MAFFT multiple sequence alignment software version 7: Improvements in performance and usability. *Molecular Biology and Evolution*, *30*, 772–780.

Kishino, H., & Hasegawa, M. (1989). Evaluation of the maximum likelihood estimate of the evolutionary tree topologies from DNA sequence data, and the branching order in hominoidea. *Journal of Molecular Evolution*, *29*, 170–179.

Kishino, H., Miyata, T., & Hasegawa, M. (1990). Maximum likelihood inference of protein phylogeny and the origin of chloroplasts. *Journal of Molecular Evolution*, *31*, 151–160.

Kozlov, A. M., Darriba, D., Flouri, T., Morel, B., & Stamatakis, A. (2019). RAxML-NG: A fast, scalable and user-friendly tool for maximum likelihood phylogenetic inference. *Bioinformatics*, *35*, 4453–4455.

Kutzbach, J. E., Guetter, P. J., Ruddiman, W. F., & Prell, W. L. (1989). The sensitivity of climate to late Cenozoic uplift in southern Asia and the American west: Numerical experiments. *Journal of Geophysical Research*, *94*, 18393–18407.

Kutzbach, J. E., Prell, W. L., & Ruddiman, W. F. (1993). Sensitivity of Eurasian climate to surface uplift of the Tibetan Plateau. *Journal of Geology*, *101*, 177–190.

Landis, M. J., Matzke, N. J., & Moore, B. R. (2013). Bayesian analysis of biogeography when the number of areas is large. *Systematic Biology*, *62*, 789–804.

Lanfear, R., Calcott, B., Kainer, D., Mayer, C., & Stamatakis, A. (2014). Selecting optimal partitioning schemes for phylogenomic datasets. *BMC Evolutionary Biology*, *14*, 82.

Li, W., & Godzik, A. (2006). Cd-hit: A fast program for clustering and comparing large sets of protein or nucleotide sequences. *Bioinformatics*, *22*, 1658–1659.

Matzke, N. (2016). *Stochastic mapping under biogeographical models*.

Matzke, N. J. (2013). Probabilistic historical biogeography: New models for founder-event speciation, imperfect detection, and fossils allow improved accuracy and model-testing. *Frontiers of Biogeography*, *5*, 242–248.

Minh, B. Q., Nguyen, M. A., & von Haeseler, A. (2013). Ultrafast approximation for phylogenetic bootstrap. *Molecular Biology and Evolution*, *30*, 1188–1195.

Minh, B. Q., Schmidt, H. A., Chernomor, O., Schrempf, D., Woodhams, M. D., von Haeseler, A., & Lanfear, R. (2020). IQ-TREE 2: New models and efficient methods for phylogenetic inference in the genomic era. *Molecular Biology and Evolution*, *37*, 1530–1534.

Molnar, P., Boos, W. R., & Battasti, D. S. (2010). Orographic controls on climate and paleoclimate of Asia: Thermal and mechanical roles for the Tibetan Plateau. *Annual Review of Earth and Planetary Sciences*, *38*, 77–102.

Molnar, P., England, P., & Martiod, J. (1993). Mantle dynamics, uplift of the Tibetan Plateau and the Indian monsoon development. *Reviews of Geophysics*, *34*, 357–396.

Mulch, A., & Chamberlain, C. P. (2006). Earth science—The rise and growth of Tibet. *Nature*, *439*, 670–671.

Mulch, A., & Chamberlain, C. P. (2018). Stable isotope Peleoaltimetry: Paleotopography as a key element in the evolution of landscape

and life. In C. Hoorn, A. Perrigo, & A. Antonelli (Eds.), *Mountains, climate and biodiversity* (pp. 81–94). Wiley & Sons.

Murphy, M. A., Yin, A., Harrison, T. M., Dürr, S. B., Chen, Z., Ryerson, F. J., Kidd, W. S. F., Wang, X., & Zhou, X. (1997). Did the indo-Asian collision alone create the Tibetan Plateau? *Geology*, *25*, 719–722.

Nogués-Bravo, D. (2009). Predicting the past distribution of species climatic niches. *Global Ecology and Biogeography*, *18*, 521–531.

Pagel, M. (1999). Inferring the historical patterns of biological evolution. *Nature*, *401*, 877–884.

Paradis, E., Claude, J., & Strimmer, K. (2004). APE: Analyses of Phylogenetics and evolution in R language. *Bioinformatics*, *20*, 289–290.

Phillips, S. J., Anderson, R. P., Dudik, M., Schapire, R. E., & Blair, M. E. (2017). Opening the black box: An open-source release of Maxent. *Ecography*, *40*, 887–893.

Phillips, S. J., & Dudík, M. (2008). Modeling of species distributions with Maxent: New extensions and comprehensive evaluation. *Ecography*, *31*, 161–175.

Phillips, S. J., Dudík, M., & Schapire, R. E. (2017). *Maxent software for modeling species niches and distributions* (Version 3.4.1). http://biodiversityinformatics.amnh.org/open_source/maxent/

Pilliod, D., McCaffery, R., Arkle, R., Scherer, R. D., Cupples, J. B., Eby, L. A., Hossack, B. R., Lingo, H., Lohr, K. N., Maxell, B. A., McGuire, M. J., Mellison, C., Meyer, M. K., Munger, J. C., Slatauski, T., & Van Horne, R. (2022). Importance of local weather and environmental gradients on demography of a broadly distributed temperate frog. *Ecological Indicators*, *136*, 108648.

Portik, D. M., Smith, L. L., & Bi, K. (2016). An evaluation of transcriptome-based exon capture for frog phylogenomics across multiple scales of divergence (Class: Amphibia, Order: Anura). *Molecular Ecology Resources*, *16*, 1069–1083.

Portik, D. M., Streicher, J. W., Blackburn, D. C., Moen, D. S., Hutter, C. R., & Wiens, J. J. (2023). Redefining possible: Combining Phylogenomic and Supersparse data in frogs. *Molecular Biology and Evolution*, *40*, msad109.

Pottier, P., Lin, H. Y., Oh, R. R. Y., Pollo, P., Rivera-Villanueva, A. N., Valdebenito, J. O., Yang, Y., Amano, T., Burke, S., Drobniak, S. M., & Nakagawa, S. (2022). A comprehensive database of amphibian heat tolerance. *Scientific Data*, *9*, 600.

Pyron, R. A. (2014). Biogeographic analysis reveals ancient continental vicariance and recent oceanic dispersal in amphibians. *Systematic Biology*, *63*, 779–797.

Pyron, R. A., & Wiens, J. J. (2013). Large-scale phylogenetic analyses reveal the causes of high tropical amphibian diversity. *Proceedings of the Biological Sciences*, *280*, 20131622.

Quade, J., Breecker, D. O., Daëron, M., & Eiler, J. (2011). The Paleoaltimetry of Tibet: An isotopic perspective. *American Journal of Science*, *311*, 77–115.

Quintero, I., & Wiens, J. J. (2013). Rates of projected climate change dramatically exceed past rates of climatic niche evolution among vertebrate species. *Ecology Letters*, *16*, 1095–1103.

Rage, J.-C., Gupta, S. S., & Prasad, G. V. R. (2016). Amphibians and squamates from the Neogene Siwalik beds of Jammu and Kashmir, India. *Paläontologische Zeitschrift*, *75*, 197–205.

Rage, J.-C., & Rocek, Z. (2007). A new species of *Thaumastosaurus* (Amphibia: Anura) from the Eocene of Europe. *Journal of Vertebrate Paleontology*, *27*, 329–336.

Rahbek, C., Borregaard, M. K., Antonelli, A., Colwell, R. K., Holt, B. G., Nogues-Bravo, D., Rasmussen, C. M. Ø., Richardson, K., Rosing, M. T., Whittaker, R. J., & Fjeldså, J. (2019). Building mountain biodiversity: Geological and evolutionary processes. *Science*, *365*, 1114–1119.

Rambaut, A., Drummond, A. J., Xie, D., Baele, G., & Suchard, M. A. (2018). Posterior summarization in Bayesian Phylogenetics using tracer 1.7. *Systematic Biology*, *67*, 901–904.

Raymo, M. E., & Ruddiman, W. F. (1992). Tectonic forcing of late Cenozoic climate. *Nature*, *359*, 117–122.

Ree, R. H., Moore, B. R., Webb, C. O., & Donoghue, M. J. (2005). A likelihood framework for inferring the evolution of geographic range on phylogenetic trees. *Evolution*, *59*, 2299–2311.

Ree, R. H., & Sanmartin, I. (2018). Conceptual and statistical problems with the DEC+J model of founder-event speciation and its comparison with DEC via model selection. *Journal of Biogeography*, *45*, 741–749.

Renner, S. S. (2016). Available data point to a 4-km-high Tibetan Plateau by 40Ma, but 100 molecular-clock papers have linked supposed recent uplift to young node ages. *Journal of Biogeography*, *43*, 1479–1487.

Revell, L. (2014). phytools 2.0: An updated R ecosystem for phylogenetic comparative methods (and other things). *PeerJ*, *12*, e16505.

Revell, L. J. (2012). Phytools: Phylogenetic tools for comparative biology (and other things). *Methods in Ecology and Evolution*, *3*, 217–223.

Revell, L. J., Harmon, L. J., & Collar, D. C. (2008). Phylogenetic signal, evolutionary process, and rate. *Systematic Biology*, *57*, 591–601.

Rodder, D., Lawing, A. M., Flecks, M., Ahmadzadeh, F., Dambach, J., Engler, J. O., Habel, J. C., Hartmann, T., Hörnes, D., Ihlow, F., Schidelko, K., Stiels, D., & Polly, P. D. (2013). Evaluating the significance of paleophylogeographic species distribution models in reconstructing quaternary range-shifts of nearctic chelonians. *PLoS One*, *8*, e72855.

Ronquist, F. (1997). Dispersal-vicariance analysis: A new approach to the quantification of historical biogeography. *Systematic Biology*, *46*, 195–203.

Ronquist, F., Teslenko, M., van der Mark, P., Ayres, D. L., Darling, A., Höhna, S., Larget, B., Liu, L., Suchard, M. A., & Huelsenbeck, J. P. (2012). MrBayes 3.2: Efficient Bayesian phylogenetic inference and model choice across a large model space. *Systematic Biology*, *61*, 539–542.

Rowley, D. B., & Currie, B. S. (2006). Palaeo-altimetry of the late Eocene to Miocene Lunpola basin, central Tibet. *Nature*, *439*, 677–681.

Schmidt, J., Bohner, J., Brandl, R., & Opgenoorth, L. (2017). Mass elevation and lee effects markedly lift the elevational distribution of ground beetles in the Himalaya-Tibet orogen. *PLoS One*, *12*, e0172939.

Schmidt, J., Opgenoorth, L., Holl, S., & Bastrop, R. (2012). Into the Himalayan exile: The phylogeography of the ground beetle Ethira clade supports the Tibetan origin of forest-dwelling Himalayan species groups. *PLoS One*, *7*, e45482.

Schmidt, J., Opgenoorth, L., Mao, K., Baniya, C. B., & Hofmann, S. (2023). Molecular phylogeny of mega-diverse *Carabus* attests late Miocene evolution of alpine environments in the Himalayan-Tibetan Orogen. *Scientific Reports*, *13*, 13272.

Schmidt, J., Opgenoorth, L., Martens, J., & Miehe, G. (2011). Neoendemic ground beetles and private tree haplotypes: Two independent proxies attest a moderate LGM summer temperature depression of 3 to 4K for the southern Tibetan Plateau. *Quaternary Science Reviews*, *30*, 1918–1925.

Shimodaira, H. (2002). An approximately unbiased test of phylogenetic tree selection. *Systematic Biology*, *51*, 492–508.

Shimodaira, H., & Hasegawa, M. (1999). Multiple comparisons of log-likelihoods with applications to phylogenetic inference. *Molecular Biology and Evolution*, *16*, 1114–1116.

Spicer, R. A. (2017). Tibet, the Himalaya, Asian monsoons and biodiversity—In what ways are they related? *Plant Diversity*, *39*, 233–244.

Spicer, R. A., Harris, N. B. W., Widdowson, M., Herman, A. B., Guo, S., Valdes, P. J., Wolfe, J. A., & Kelley, S. P. (2003). Constant elevation of southern Tibet over the past 15 million years. *Nature*, *421*, 622–624.

Spicer, R. A., Su, T., Valdes, P. J., Farnsworth, A., Wu, F. X., Shi, G., Spicer, T. E. V., & Zhou, Z. (2021a). The topographic evolution of the Tibetan region as revealed by palaeontology. *Palaeobiodiversity and Palaeoenvironments*, *101*, 213–243.

Spicer, R. A., Su, T., Valdes, P. J., Farnsworth, A., Wu, F. X., Shi, G., Spicer, T. E. V., & Zhou, Z. (2021b). Why 'the uplift of the Tibetan Plateau' is a myth? *National Science Review*, *8*, 1–19.

Stamatakis, A. (2014). RAxML Version 8: A tool for phylogenetic analysis and post-analysis of large phylogenies. *Bioinformatics*, *30*, 1312–1313.

Strimmer, K., & Rambaut, A. (2002). Inferring confidence sets of possibly misspecified gene trees. *Proceedings of the Royal Society B: Biological Sciences*, *269*, 137–142.

Su, T., Farnsworth, A., Spicer, R. A., Huang, J., Wu, F. X., Liu, J., Li, S. F., Xing, Y. W., Huang, Y. J., Deng, W. Y. D., Tang, H., Xu, C. L., Zhao, F., Srivastava, G., Valdes, P. J., Deng, T., & Zhou, Z. K. (2019). No high Tibetan Plateau until the Neogene. *Science Advances*, *5*, eaav2189.

Sun, J., Xu, Q., Liu, W. Z., Zhang, Z., Xue, L., & Zhao, P. (2014). Palynological evidence for the latest Oligocene-early Miocene paleoelevation estimate in the Lunpola Basin, central Tibet. *Palaeogeography, Palaeoclimatology, Palaeoecology*, *399*, 21–30.

Sun, Y. B., Fu, T. T., Jin, J. Q., Murphy, R. W., Hillis, D. M., Zhang, Y. P., & Che, J. (2018). Species groups distributed across elevational gradients reveal convergent and continuous genetic adaptation to high elevations. *Proceedings of the National Academy of Sciences of the United States of America*, *115*, E10634–E10641.

Sun, Y. B., Liang, Y., Liu, H. Q., Liu, J., Ji, J., Ke, X., Liu, X., He, Y., Wang, H., Zhang, B., Zhang, Y., Zhuang, G., Pei, J., Li, Y., Quan, C., Li, J., Aitchison, J. C., Liu, W., & Liu, Z. (2023). Mid-Miocene sea level altitude of the Qaidam Basin, northern Tibetan Plateau. *Communications Earth & Environment*, *4*, 3.

Tapponnier, P., Xu, Z. Q., Roger, F., Meyer, B., Arnaud, N., Wittlinger, G., & Jingsui, Y. (2001). Oblique stepwise rise and growth of the Tibet plateau. *Science*, *294*, 1671–1677.

Visser, M. E. (2008). Keeping up with a warming world; assessing the rate of adaptation to climate change. *Proceedings of the Biological Sciences*, *275*, 649–659.

Wang, B., Xie, F., Li, J., Wang, G., Li, C., & Jiang, J. (2017). Phylogeographic investigation and ecological niche modelling of the endemic frog species Nanorana pleskei revealed multiple refugia in the eastern Tibetan Plateau. *PeerJ*, *5*, e3770.

Wang, C., Zhao, X., Liu, Z., Lippert, P. C., Graham, S. A., Coe, R. S., Yi, H., Zhu, L., Liu, S., & Li, Y. (2008). Constraints on the early uplift history of the Tibetan Plateau. *Proceedings of the National Academy of Sciences*, *105*, 4987–4992.

Wang, C. S., Dai, J., Zhao, X., Li, Y., Graham, S. A., He, D., Ran, B., & Meng, J. (2014). Outward-growth of the Tibetan Plateau during the Cenozoic: A review. *Tectonics*, *621*, 1–43.

Wang, Y., Deng, T., & Biasatti, D. (2006). Ancient diets indicate significant uplift of southern Tibet after ca. 7 Ma. *Geology*, *34*, 309–312.

Wiens, J. J. (2011). The niche, biogeography and species interactions. *Philosophical Transactions of the Royal Society, B: Biological Sciences*, *366*, 2336–2350.

Wiens, J. J., Ackerly, D. D., Allen, A. P., Anacker, B. L., Buckley, L. B., Cornell, H. V., Damschen, E. I., Jonathan Davies, T., Grytnes, J. A., Harrison, S. P., Hawkins, B. A., Holt, R. D., McCain, C. M., & Stephens, P. R. (2010). Niche conservatism as an emerging principle in ecology and conservation biology. *Ecology Letters*, *13*, 1310–1324.

Wiens, J. J., & Donoghue, M. J. (2004). Historical biogeography, ecology and species richness. *Trends in Ecology & Evolution*, *19*, 639–644.

Wiens, J. J., & Graham, C. H. (2005). Niche conservatism: Integrating evolution, ecology, and conservation biology. *Annual Review of Ecology, Evolution, and Systematics*, *36*, 519–539.

Wiens, J. J., Graham, C. H., Moen, D. S., Smith, S. A., & Reeder, T. W. (2006). Evolutionary and ecological causes of the latitudinal diversity gradient in hylid frogs: Treefrog trees unearth the roots of high tropical diversity. *The American Naturalist*, *168*, 579–596.

Wu, F., Miao, D., Chang, M. M., Shi, G., & Wang, N. (2017). Fossil climbing perch and associated plant megafossils indicate a warm and wet central Tibet during the late Oligocene. *Scientific Reports*, *7*, 878.

Wuertz, D., Setz, T., Chalabi, Y., Boudt, C., Chausse, P., & Miklovac, M. (2019). *fGarch: Rmetrics—Autoregressive conditional heteroskedastic modelling*. R package version 3042.83.1. https://CRAN.R-project.org/package=fGarch

Xu, J., Badola, R., Chettri, N., Chaudhary, R. P., Zomer, R., Pokhrel, B., Hussain, S. A., Pradhan, S., & Pradhan, R. (2019). Sustaining biodiversity and ecosystem Services in the Hindu Kush Himalaya. In P. Wester, A. Mishra, A. Mukherji, & A. Shrestha (Eds.), *The Hindu Kush Himalaya assessment* (pp. 127–165). Springer, Cham.

Yin, J., Zhang, C., & Mirarab, S. (2019). ASTRAL-MP: Scaling ASTRAL to very large datasets using randomization and parallelization. *Bioinformatics*, *35*, 3961–3969.

Zhang, J., Kapli, P., Pavlidis, P., & Stamatakis, A. (2013). A general species delimitation method with applications to phylogenetic placements. *Bioinformatics*, *29*, 2869–2876.

Zhang, R., Jiang, D. B., Ramstein, G., Zhang, Z., Lippert, P. C., & Yu, E. (2018). Changes in Tibetan Plateau latitude as an important factor for understanding east Asian climate since the Eocene: A modeling study. *Earth and Planetary Science Letters*, *484*, 295–308.

Zhou, W. W., Zhang, B. L., Chen, H. M., Jin, J. Q., Yang, J. X., Wang, Y. Y., Jiang, K., Murphy, R. W., Zhang, Y. P., & Che, J. (2014). DNA barcodes and species distribution models evaluate threats of global climate changes to genetic diversity: A case study from *Nanorana parkeri* (Anura: Dicroglossidae). *PLoS One*, *9*, e103899.

Zhou, Z., Yang, Q., & Xia, K. (2007). Fossils of *Quercus* sect. *Heterobalanus* can help explain the uplift of the Himalayas. *Chinese Science Bulletin*, *52*, 238–247.

## SUPPORTING INFORMATION

Additional supporting information can be found online in the Supporting Information section at the end of this article.

**How to cite this article:** Hofmann, S., Rödder, D., Andermann, T., Matschiner, M., Riedel, J., Baniya, C. B., Flecks, M., Yang, J., Jiang, K., Jianping, J., Litvinchuk, S. N., Martin, S., Masroor, R., Nothnagel, M., Vershinin, V., Zheng, Y., Jablonski, D., Schmidt, J., & Podsiadlowski, L. (2024). Exploring Paleogene Tibet's warm temperate environments through target enrichment and phylogenetic niche modelling of Himalayan spiny frogs (Paini, Dicroglossidae). *Molecular Ecology*, *33*, e17446. https://doi.org/10.1111/mec.17446